You Can't Run, but You Can Hide: The Skeleton of the Sand-Swimmer Lizard *Calyptommatus leiolepis* (Squamata: Gymnophthalmidae)

NICHOLAS T. HOLOVACS,¹ JUAN D. DAZA ¹O,^{1*} CECILIA GUERRA,² EDWARD L. STANLEY,³ AND RICARDO MONTERO ¹O²

¹Department of Biological Sciences, Sam Houston State University, Huntsville, Texas
²Cátedra Vertebrados, Facultad de Ciencias Naturales, Universidad Nacional de Tucumán, Instituto de Herpetología, Fundación Miguel Lillo, Tucumán, Argentina
³Department of Herpetology, Florida Museum of Natural History, Gainesville, Florida

ABSTRACT

Squamates exhibit a vast diversity of body plans, which directly determines habitat use and preference. Here the skeleton of the sand-swimmer burrower gymnophthalmid, Calyptommatus leiolepis, is analyzed to investigate how its peculiar fossorial locomotion affects its osteology. Calyptommatus leiolepis is a limb-reduced, short-intermediate tailed lizard. Although there are other studies on its general anatomy, we performed a detailed description of its skeleton. Using high-resolution computer tomography, each bone element within the skeleton was digitally segmented and a detailed description rendered. Anatomical features related to burrowing include the head having a shovel-like snout with a well-developed horizontal soft tissue ridge, nasal cartilages that exclude sand from the nostrils, reduced eyes covered by a brille, lack of forelimbs, extreme reduction of hind limbs, and imbricated scales among others. The genus Calyptommatus has unique features such as a triradiate jugal (with digit-like posterior projections), a reduced pectoral girdle and forelimbs, parasternal processes that interconnect the ribs, and a single digit in the hind limbs. When comparing this species with other gymnophthalmid lizards including, fossorial species, it is clear that Calyptommatus exhibits the highest number of structural modifications within the family. Despite its specialized morphology, it still retains characters that link this genus to other members of Gymnophthalmidae when included in a phylogeny based solely on phenotypic data. Anat Rec, 00:000-000, 2019. © 2019 American Association for Anatomy

Key words: microteiid; HRCT; osteology; morphology

The Order Squamata (lizards, amphisbaenians, and snakes), with more than 10,000 extant species recognized (Uetz et al., 2019), includes a diversity of body forms ranging from the typical lizard morphotype with well-developed limbs to the elongated limbless form of snakes

(Bradley et al., 2008; Vitt and Caldwell, 2014). Although the snakes constitutes 35.5% (3,763 extant species) of the total number of squamate species, the percentage of snake-like squamates is much higher because body elongation and limb/attenuation/loss has appeared in several

Grant sponsor: National Science Fundation; Grant number: (NSF) DEB 1657648..

*Correspondence to: Juan D. Daza, Department of Biological Sciences, Sam Houston State University, Huntsville, TX.

E-mail: juand.daza@gmail.com

Received 23 March 2019; Revised 14 May 2019; Accepted 24 June 2019.

DOI: 10.1002/ar.24246 Published online 00 Month 2019 in Wiley Online Library (wileyonlinelibrary.com).

extant groups, including dibamids (Anelytropsis, Dibamus), gekkotans (pygopods), scincids (e.g., Chalcides), cordylids (e.g., Chamaesaura), Gymnophthalmidae (e.g., Bachia, Calyptommatus, Nothobachia), amphisbaenians, and anguids (e.g., Ophisaurus, Ophiodes) (Gans, 1975; Rodrigues, 1991; Lee, 1998; Wiens and Slingluff, 2001; Kearney and Stuart, 2004; Conrad, 2008; Zaher et al., 2009).

Elongation of the body and reduction of limbs have been reported to be highly correlated (Presh, 1975; Wiens et al., 2006), and it was argued that they were guided by a common developmental mechanism (Greene and Cundall, 2000; Wiens and Slingluff, 2001). However, this association has been refuted and its co-occurrence explained as the result of constraints-imposed biomechanics of locomotion and common patterns of environmental selection, yet involving changes in quite separated. dissociated developmental mechanisms in each lineage (Sanger and Gibson-Brown, 2004; see also Wiens, 2004). The independence of these two traits is consistent with the observed different patterns of body elongation and limb reduction in squamates (Bradley et al., 2008). It also applies to cases in which limb reduction occurs whether the body is elongated or not, or the contrasting condition of fully limbed elongated body forms (e.g., some species in the skink genus Lygosoma).

Limb reduction in squamates has occurred several times (at least 62 times in 53 independent lineages, Greer, 1991), and most of these forms fit in two ecomorphs, a long-tailed surface dweller or a short-tailed burrowing ecomorph (Wiens et al., 2006; Bradley et al., 2008). Among gymnophthalmids that show limb reduction, there are two extreme morphologies when considering tail length: (1) forelimbs greater in size than the hind limbs and with a very long tail (e.g., Bachia) and (2) forelimbs missing and hindlimbs reduced, and with a short tail (e.g., Calyptommatus) (Rodrigues, 1991; Pellegrino et al., 2001; Jerez et al., 2010). In between these extremes, there is a wide range of variation on digit morphology and phalangeal formulae (Roscito et al., 2014), and limb attenuation, especially in the genus Bachia, which is strongly correlated with the increase of presacral vertebrae (i.e., forelimb and hindlimbs become shorter as the number of presacral vertebrae increases, Presh, 1975).

Calyptommatus leiolepis has reduced limbs, a moderately short tail, and it has an increased number of presacral vertebrae when compared with fully limbed members of Gymnophthalmoidea (sensu Goicoechea et al., 2016; Alopoglossidae, Gymnophthalmidae, Teiidae). Calyptommatus leioleopis has 44 presacral vertebrae, while limbed forms vary between 26 and 28 (Daza et al., 2018; however, see the extreme variation in the genus Bachia where the presacral number fluctuates from 25 to 53; Presh, 1975). In spite of the long trunk in C. leioleopis, its body does not reach the elongation achieved by extreme serpentiform squamates such as snakes, pygopods, amphisbaenians, some scincoids and anguimorph lizards (Hoffstetter and Gasc, 1969; Daza et al., 2018). This combination of traits might presuppose a limitation in locomotion in land (e.g., concertina locomotion), but this body form allows the species to sand-swim in the loose sandy habitats of the inner dunes of the São Francisco River, Bahia, Brazil (Rodrigues, 1991; Lambertz, 2010; Siedchlag et al., 2010). In addition to the reduction of limbs, this species has developed other adaptations for sand-swimming such as the development of a head with a transverse "shovel-like" snout, fusion of the head scales, eyes covered by a brille, and an inverted U-shaped body that allows sand to go under the abdomen (as in trogonophid amphisbaenians such as *Agamodon*, R. Montero, personal observation).

There are four species in the genus Calyptommatus, and their relationship with other gymnophthalmids was determined using molecular data (Pellegrino et al., 2001; Pyron et al., 2013; Goicochea et al., 2016). Roscito and Rodrigues (2010) described in detail the cranial osteology C. nicterus together with Scriptosaura catimbau and Nothobachia ablephara: the three species are highly fossorial and share similar morphological traits that may be related to their mode of life. A redescription of the cranial anatomy of the genus Calyptommatus is unnecessary at this point. Instead, we will be referring only to aspects that need to be explored more in detail, indicating some characteristics that might have some phylogenetic value. For a more generalized description of the genus Calyptommatus, we refer the reader to the paper by Roscito and Rodrigues (2010). Here, new details are provided about the internal anatomy of the skull based on high-resolution X-ray computed tomography (HRCT). Finally, we contrasted the species studied herein with available descriptions of other squamates that have similar life modes. Morphological data collected were used to test the phylogenetic position using morphology of this highly derived fossorial lizard within the framework of squamata.

MATERIALS AND METHODS

Five specimens of *Calyptommatus leiolepis* from the Fundación Miguel Lillo, San Miguel de Tucumán (FML), were prepared using different techniques, including clearing and staining, skeletonization, and micro-CT (Fig. 1). Three specimens (FML 30529, FML 30530, and FML 30533) were cleared and double stained using the protocol of Maisano (2008). Each of the staining reagents was gradually increased in concentration until cartilage or bone, depending on the reagent, were clearly visible through the soft tissue. Two additional specimens (FML 30531–30532) were skeletonized using fine pointed tweezers and cleaned slowly with a 1:100 dilution of 5% sodium hypochlorite.

MicroCT data were obtained from a cleared and stained specimen (FML 30533) at the American Museum of Natural History in New York using a GE Phoenix v|tome|x s240 system with a molybdenum target and modification of the current and voltage to maximize the range of densities recorded. Image stacks were used to create threedimensional models of the entire animal skeleton. This imaging technology allows a comprehensive look at the osteological and soft tissue anatomy without harming the integrity of the specimen, and to our knowledge, this is the first time that a cleared and stained specimen has been scanned. Using the computer software Avizo Lite v. 9.5.0 (© FEI SAS, Thermo Fisher Scientific, 2018), the image stack consisting of 8-bit TIFF files were loaded into the program to segment individual bones. Voxel values for X, Y, and Z were 0.01427314, and were made available at Morphosource (https://www.morphosource.org/Detail/MediaDetail/ Show/media_id/45057). Each bone of the skull, selected vertebrae to indicate regional variation, and appendicular skeleton were digitally segmented.

One specimen of *C. leiolepis* (FML 30530) was photographed using a NIXON E4300 camera and illustrated in

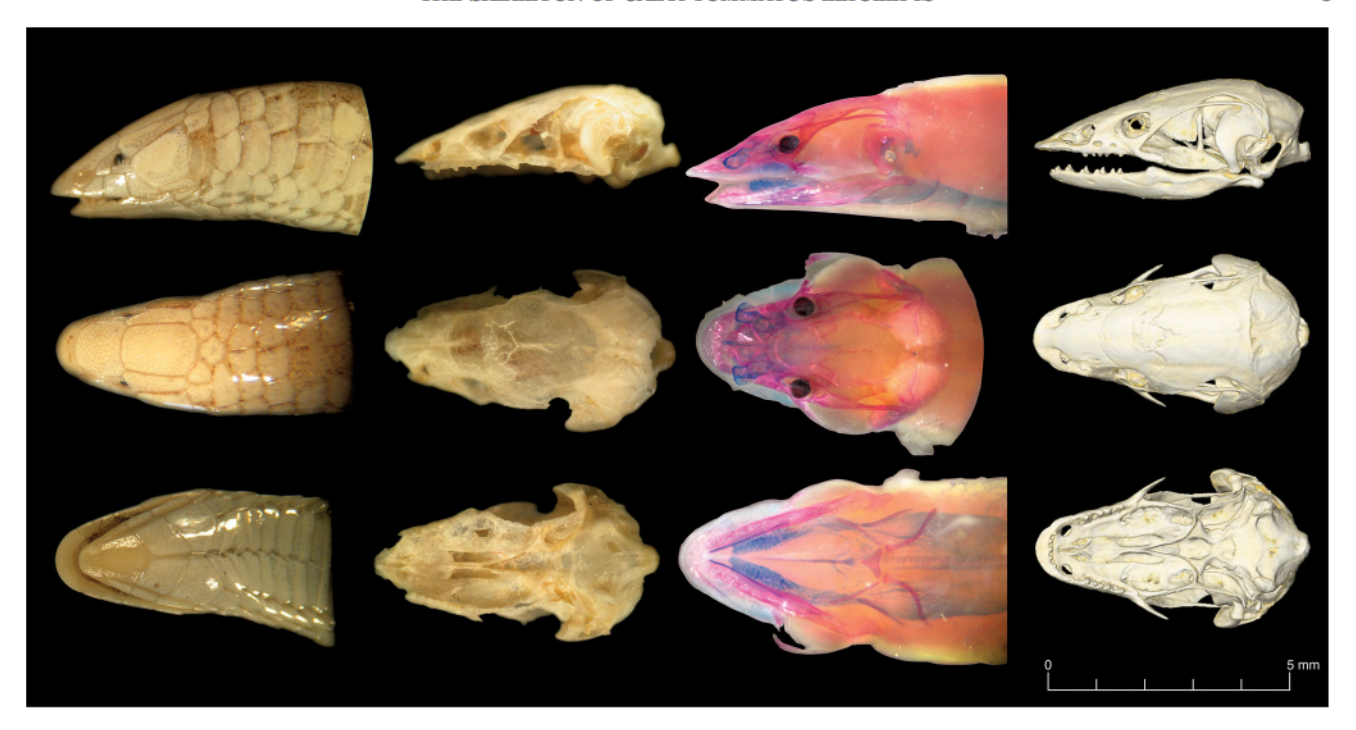


Fig. 1. Lateral, dorsal, and ventral views of four preparations of *Calyptommatus leiolepis* specimens: whole-body dissection (FML 30533), dried skeleton (FML 30531), cleared and stained, and HRCT segmentation (FML 30530).

Adobe Illustrator (Adobe Creative Cloud Illustrator CC, 2018), tracing directly onto the digital photographs. The illustration represents overlapped bone sutures with dashed lines, bone colored as white, and cartilage as blue (Fig. 2).

To test the phylogenetic position of C. leiolepis, morphological data for this species were retrofitted into a large morphological dataset of squamate reptiles (Gauthier et al., 2012). This data set included 193 taxa and 610 characters that were composed of both cranial and postcranial osteology as well as a number of soft anatomy characters. Morphological characters were scored using observations made from the HRCT scans, cleared and stained specimens, ethanol-preserved specimens, and skeletonized specimens. Each character was coded quantitatively in a binary or multistate manner. Morphological characters were entered in the data management and processing software, Mesquite v. 3.40 (Maddison and Maddison, 2018). After characters were entered in Mesquite v. 3.40, the file was exported in TNT format. Characters were ordered as in Gauthier et al. (2012). The analysis using Maximum Parsimony treated all characters equally weighted. Analysis was run in TNT v. 1.5 (Goloboff and Catalano, 2016). Phylogenetic analysis used new technology options, 50 independent searches that include a combination of sectorial search (RSS, CSS, 3 changes in sectors of size below 75, and 10 changes in sectors of size above 75) and tree fusing (three rounds, swap after exchanging, start from best tree, and use fusing to multiply optimal trees). Sphenodon punctatus was used to root the tree, and the ingroup was formed by only squamate taxa. After the search was completed, a strict consensus tree was calculated and Relative Bremer, Bremer, and Bootstrap support (100 pseudoreplicates) were used as measures of node support.

RESULTS

The skull of *Calyptommatus leiolepis* is miniaturized (FML 30530 ~ 6.8 mm in length), longer than wide, with a rounded and depressed snout (Fig. 2A–C). There is an anterior rim of connective tissue that is attached to the premaxilla, maxilla and jugal (Fig. 3), making the snout wider, although the bony is narrow. The rim of connective tissue forms a sharp horizontal keel that extends anteriorly beyond the lower jaw, placing the mouth in a ventral position, and creating a lateral and flattened extension of the snout with a "lip" that produces the impression of an overbite. The anterorbital snout is shortened, and the nares open laterally and are protected anteriorly by cartilaginous nasal flaps similar to fenders that are external projections of the nasal cartilages preventing soil particles from entering the nasal cavity (Fig. 3).

The orbit is small and complete posteriorly, being surrounded by the prefrontal, jugal, postorbitofrontal, maxilla, and frontal bones (Fig. 4A). The orbit has a diameter that is about 11% of the total skull length, opens almost dorsally. The frontoparietal suture is located about midway along the length of the skull length (Fig. 4B). In gymnophthalmids, the mesokinetic plane at the frontoparietal suture is reinforced by means of the interlocked paired frontal tabs that overlap the parietal anterior edge but also by an additional posteromedial frontal process that is wedged into the parietal (Arnold, 1998; Bell et al., 2003; Evans, 2008) (Fig. 4B). In C. leiolepis the posteromedial process of the frontal invades the interparietal suture (Fig. 4B). This reinforcement of the skull at the frontoparietal suture is also developed by other means (e.g., interdigitated sutures) in other members of the Lacertoidea (e.g., teiids, lacertids, amphisbaenians; Müller et al., 2011; Gauthier et al., 2012),

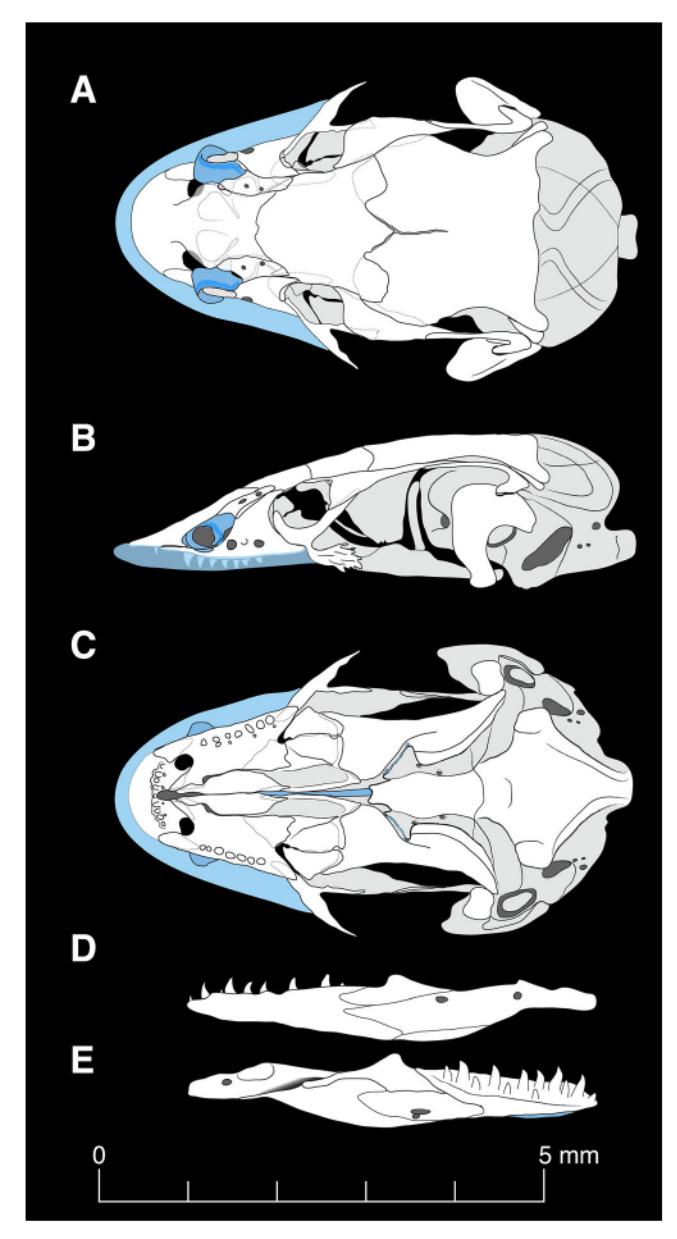
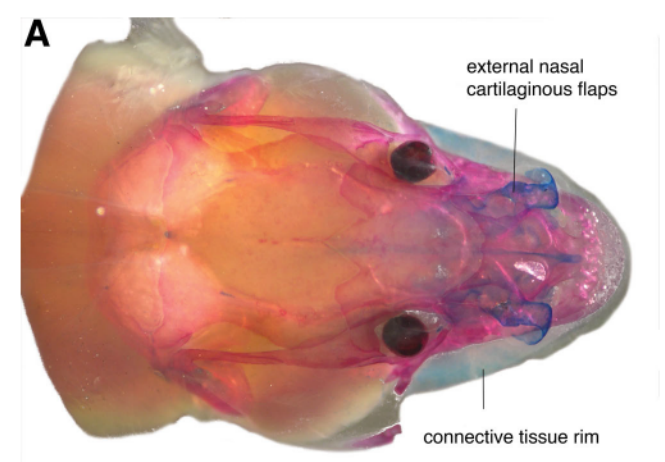


Fig. 2. Illustration of the skull of *Calyptommatus leiolepis* (FML 30530) in dorsal **(A)**, lateral **(B)**, and ventral **(C)** views; and the left jaw in lateral **(D)** and medial **(E)** views. Dashed lines represent the overlapping of bone, white/light gray color is bone, and blue color is cartilage.

which might indicate a trend toward skull reinforcement in this lizard clade.

In miniaturized gymnophthalmoideans, as in other lizards, the basicranium is proportionally wide, especially in the area occupied by the otic capsules (Rieppel, 1984a). The occiput in miniaturized gymnophthalmoideans is globular and not covered by the parietal, having a bulging occipital condyle (Fig. 4A–C; Hernández Morales et al., 2019).

The skull is wedge-shaped and compact (Fig. 4A). Posterior to the postorbital bar, there is a wide infratemporal recess and a much smaller supratemporal fenestra, but neither is reduced or closed as is common in miniaturized species (M. C. Vallejo, personal communication). In ventral



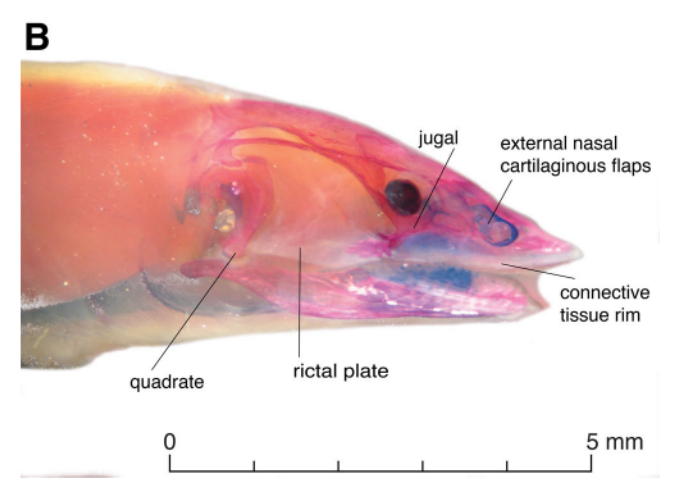


Fig. 3. Cleared and stained *Calyptommatus leiolepis* (FML 30530) in dorsal **(A)** and left lateral **(B)** views emphasizing the broad and flattened snout with a cartilaginous rim, external nasal cartilaginous flaps that cover the nasal openings, cartilaginous jugal attachments.

view, an oval and elongated premaxilla-vomer fenestra is visible (Fig. 4C). The tooth arcade develops a well-defined gap or diastema, which is formed by a short portion of the premaxilla (approximately one tooth position of space) and an anterior toothless portion of the maxilla (Fig. 4C). The formation of this diastema is possibly due to the extensive suture overlap between the premaxilla and maxilla. There is also a circular premaxillary-maxillary fenestra between these two bones (Fig. 4C). The fenestra vomeronasalis is very small and notably shifted medially as consequence of the greater development of the maxillary palatal shelf. Calyptommatus leolepis has the paleochoanate condition (Lakjer, 1927; Rieppel et al., 2008) having a fenestra vomeronasalis partially separated from the fenestra exochoanalis, but the vomer and maxilla fail to contact each other. The palate is duplicipalatinate, with a very deep choanal groove along the palatine and that forms a secondary palate partially covered by bone and cartilage. The suborbital fenestra is very small (almost closed) and irregular in shape (Fig. 4C). The interpterygoid vacuity is also greatly reduced by the anterior extension of the parabasisphenoid and the closeness of the palatines: this space is limited to a narrow slit occupied by the cartilaginous cultriformis

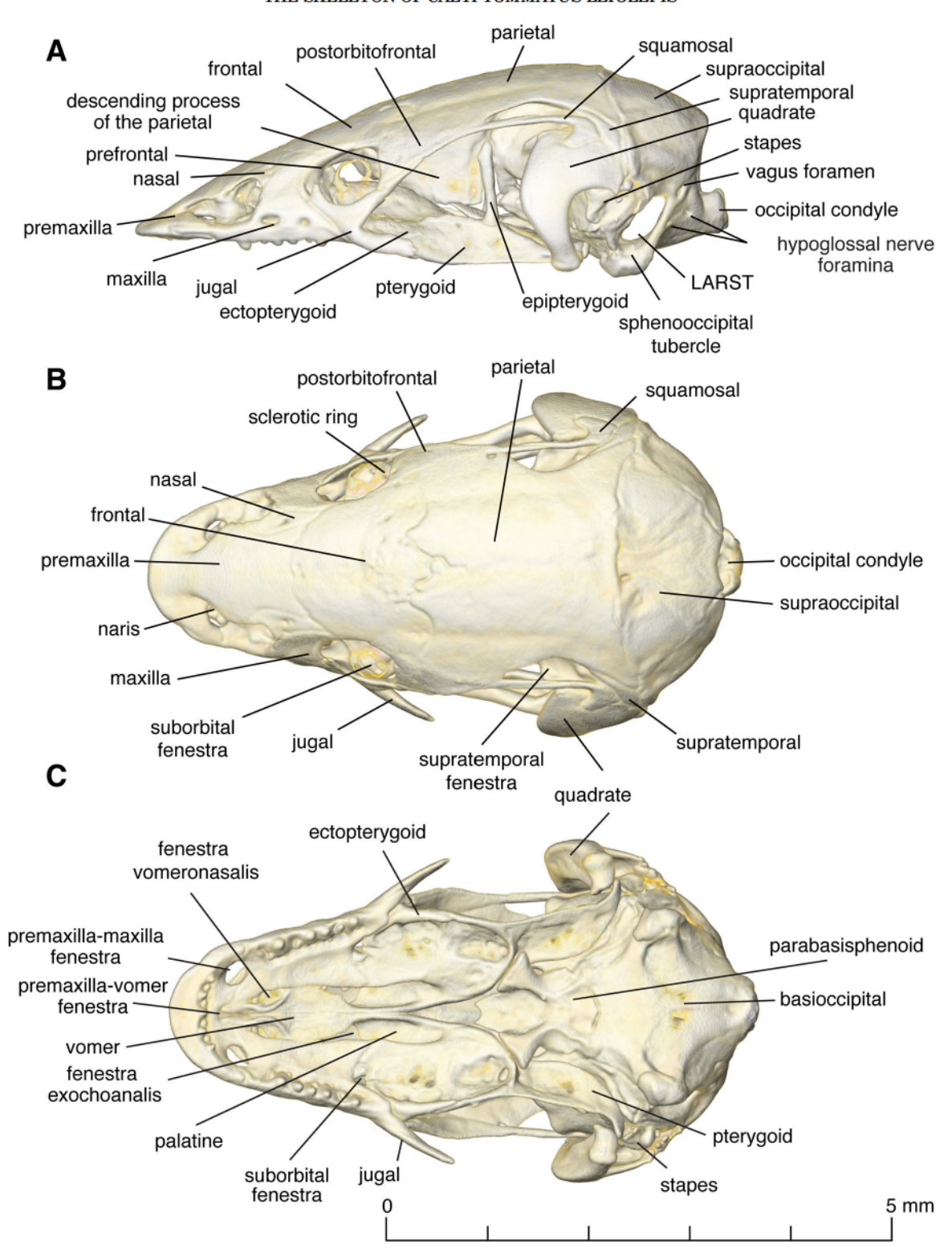


Fig. 4. HRCT of the cranium of Calyptommatus leiolepis (FML 30530) in lateral (A), dorsal (B), and (C) ventral views.

process. The posterior process of the pterygoid also develops medial plates that form a floor for the recesus vena jugularis. The pterygoid is fixed, indicating the reduced mobility of the palate, although the caps of the basipterygoid processes are still cartilaginous, indicating the presence of a synovial joint with the braincase.

The vertebral column shows regionalization, with distinct vertebrae on the cervical, thoracic, lumbar, sacral,

and caudal segments. In general, the neural arches are pointed and posterodorsally inclined, attaining the largest height in mid-thoracic region and tend to become shorter toward the caudal region. There is only one dorsal vertebra with no ribs, identified as lumbar. Both pectoral and pelvic girdles are present, and the forelimb is much reduced than the hind limb.

Individual Bone Descriptions

Premaxilla. The nasal process of the premaxilla contacts the nasals laterally, the frontal posterodorsally, and the vomer posteroventrally (Figs. 4B and 5A). This process is wide and long, having a complex shape, and being the most prominent element of the snout (Fig. 6A-E). It forms the dorsolateral border of the naris, roofing the most part of the nasal cavity and the septomaxilla. This bone bears nine teeth that are attached toward the posterior edge of the palatal shelf (Figs. 4C and 6B, E). As a consequence of not being attached to the margin of the tooth arcade, the tooth implantation is pleurodont, but the medial wall of the premaxillary parapet is very low, and it renders a view that makes tooth implantation almost acrodont. The premaxilla contacts the maxillary lappets, and the anterior processes of the vomer separate the maxillae and contact briefly the premaxilla. The premaxilla palatal shelf is indented and forms the anterior margin of the premaxillary-vomer fenestra. There is an elongated and shallow notch nested within the lateral process of the premaxilla that receives the anterior process of the maxilla (Fig. 6A-E).

Maxilla. This bone has a tall facial process with a steep incline behind the nares (Fig. 6F-H). This process is concave posteriorly, forming part of the margin of the eye socket. The facial process is located on the posterior portion of the bone and is pierced by two to three large vascular foramina through which runs the terminal branches of the maxillary artery and the maxillary branch of cranial nerve V exit to the nasal capsule (Figs. 4A and 6F, see also Oelrich, 1956; Evans, 2008). This bone together with the frontal entirely overlap the prefrontal; therefore, it is not visible dorsally (Fig. 4A, B). The palatal shelf is very broad and almost rectangular in shape (Fig. 6J). It bears six pleurodont teeth, the same number as in C. nicterus (Figs. 4C and 6H; see also Roscito and Rodrigues, 2010). Some of the maxillary teeth are almost twice the size of the premaxillary teeth (Fig. 4C). The palatal shelf forms the posterior margin of the premaxilla-maxilla aperture, participates briefly in the premaxillary-vomer fenestra, forms the anterior margin of the fenestra vomeronasalis, the lateral margin of the fenestra exochoanalis, and the anterior the suborbital fenestra. Specifically, anteromedial and anterior process aid in the formation of the posterior margin of the premaxilla-maxilla aperture (Figs. 4C and 6G, H). In addition, the posteromedial and posterior process of the maxillary shelf come in contact with the palatine and ectopterygoid, respectively (Fig. 4C). The osseous naris edge is concave, abutting against the nasal and aiding in the formation of the posterior edge of the naris (Fig. 4A, B).

Nasal. This bone is very thin and subtriangular in shape, with a concave anterior margin and a blunt posterior margin (Figs. 4A, B and 6I, J). It forms the dorsal wall

of the nasal capsule. This bone has extensive, slightly overlapping contact with the premaxilla (medially) via the premaxilla facet and the maxilla (laterally) via the maxilla facet (Figs. 4B and 6I, J). It also overlaps the anterolateral process of the frontal bone and a small part of the prefrontal. The nasal bones bear from one to three vascular foramina, which in some specimens may be asymmetrical. The osseous naris edge aids in the posterodorsal margin of the external nares (Figs. 4A and 6I, J).

Prefrontal. In *C. leiolepis*, this bone is almost completely concealed by the facial processes of the maxilla and the jugal (Fig. 4A, B). The prefrontal has a dorsal process that extends posteriorly beneath the frontal bone: it forms most of the inner anterodorsal wall of the orbit, while the anterodorsal orbital rim is formed mostly by the maxilla and the frontal (Figs. 4A, B and 6K–N). The prefrontal contacts the nasal ventrally but in lateral view the terminus of the facial process of the maxilla separates the prefrontal from the nasal (Fig. 4A). In *C. nicterus* (Roscito and Rodrigues, 2010), the prefrontal is not visible in dorsal view, whereas in *C. leiolepis*, this bone is slightly visible (Fig. 4B).

Postorbitofrontal. The only element on the posterodorsal border of the orbit in Calyptommatus is formed by the fusion of the postfrontal and the postorbital (Figs. 4A. B and 6O. P. Roscito and Rodrigues, 2010. 2012). The squamosal makes contact with this bone on the dorsal edge via the squamosal facet (Figs. 4A, B and 6O, P). Some specimens present a small foramen in this bone, which supports observations by Roscito and Rodrigues (2010), the same argument was used to support the idea of the fusion of postfrontal and postorbital in pygopodids (Rieppel, 1984b). This bone is wide and tapers posteriorly where it contacts the squamosal to form the upper temporal bar. This bone forms the posterodorsal portion of the orbit (with the aid of the anterior process, lateroventral process, and the ridge that connects the two) and clasps the frontoparietal suture (Figs. 4A and 6O, P).

Jugal. The jugal bone is curved and has a triradiate shape as in *C. nicterus*, which appears to be a synapomorphy of the genus. It is formed by a dorsal postorbitofrontal process that contribute to the postorbital bar, an anterior maxillary process, and a posterior process (Figs. 4A–C and 6Q). The posterior process is expanded posteriorly and, in some specimens, may present digit-like posterior projections and some sculpturing (Figs. 4A and 6Q). The posterior process has a dual function, serving for the anterior attachment site of the rim of connective tissue to the snout, and posteriorly for the ligamentous rictal plate that links the jugal with the anterior margin of the quadrate (Fig. 3B).

Frontal. This bone is crown-shaped, having an anterior end that is half the width of the posterior end. Calyptommatus does not present the interorbital constriction or the anterolateral and anteromedial processes seen in other gymnophthalmid genera, but it resembles other limb-reduced forms where the frontal tends to have parallel margins. In C. leiolepis, there is a posteromedial process that invades and separates the parietals anteriorly (Figs. 2A, 4B, and 6R, S): this process is not present in C. nicterus, which presents a straight medial margin. This bone also exhibits parietal tabs in the posterior region

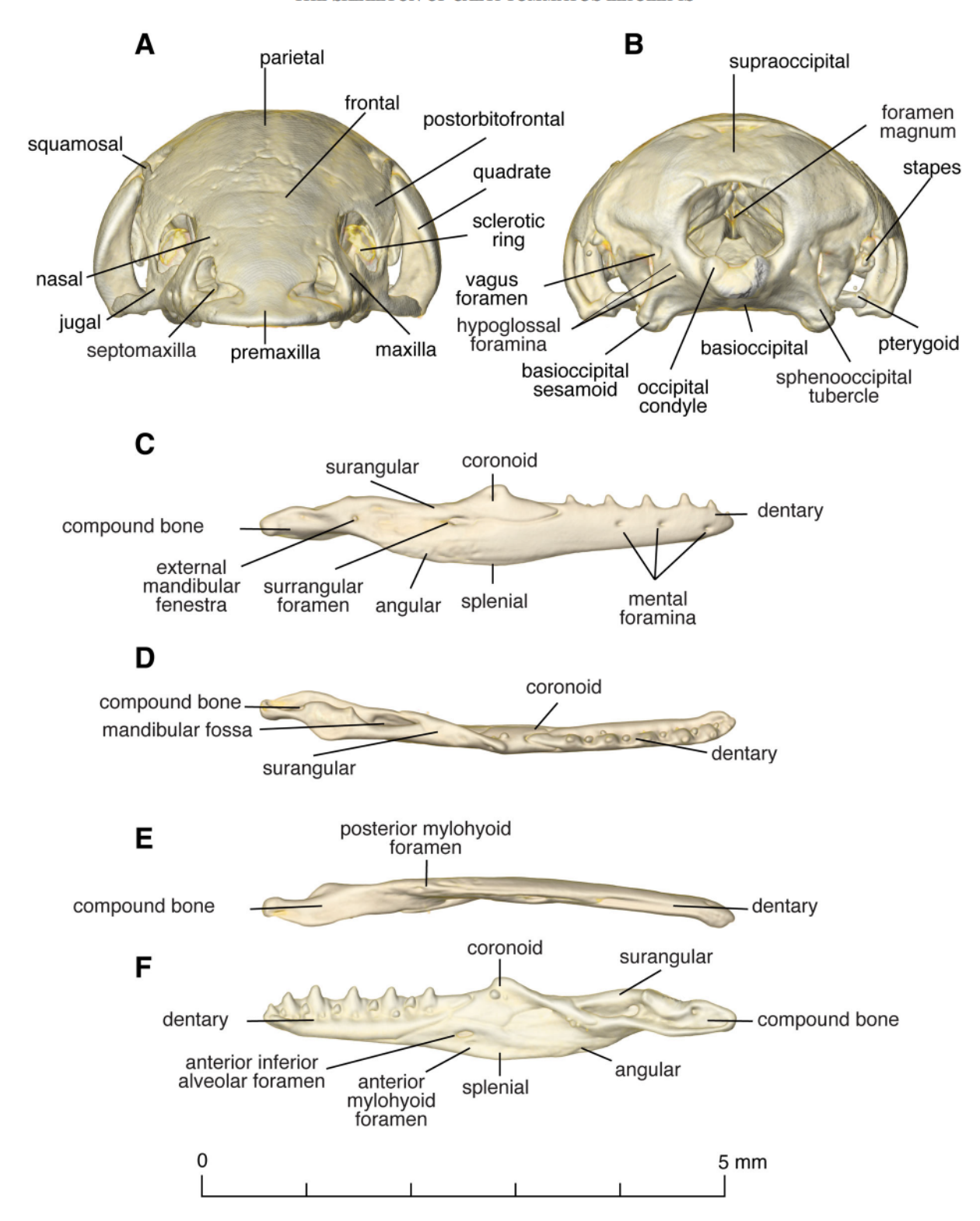


Fig. 5. HRCT of the skull of Calyptommatus leiolepis (FML 30530) in (A) anterior, and (B) posterior, views. Jaw in (C) lateral, (D) dorsal, (E) ventral, and (F) medial views.

that aid in forming a supporting structure (Figs. 4B and 6R, S). The frontal participates in forming the orbitonasal fenestra along with the palatine and the prefrontal. It also

contains laminar descending processes (crista cranii) protects the olfactory tracts without joining ventrally (Fig. 6R, S).

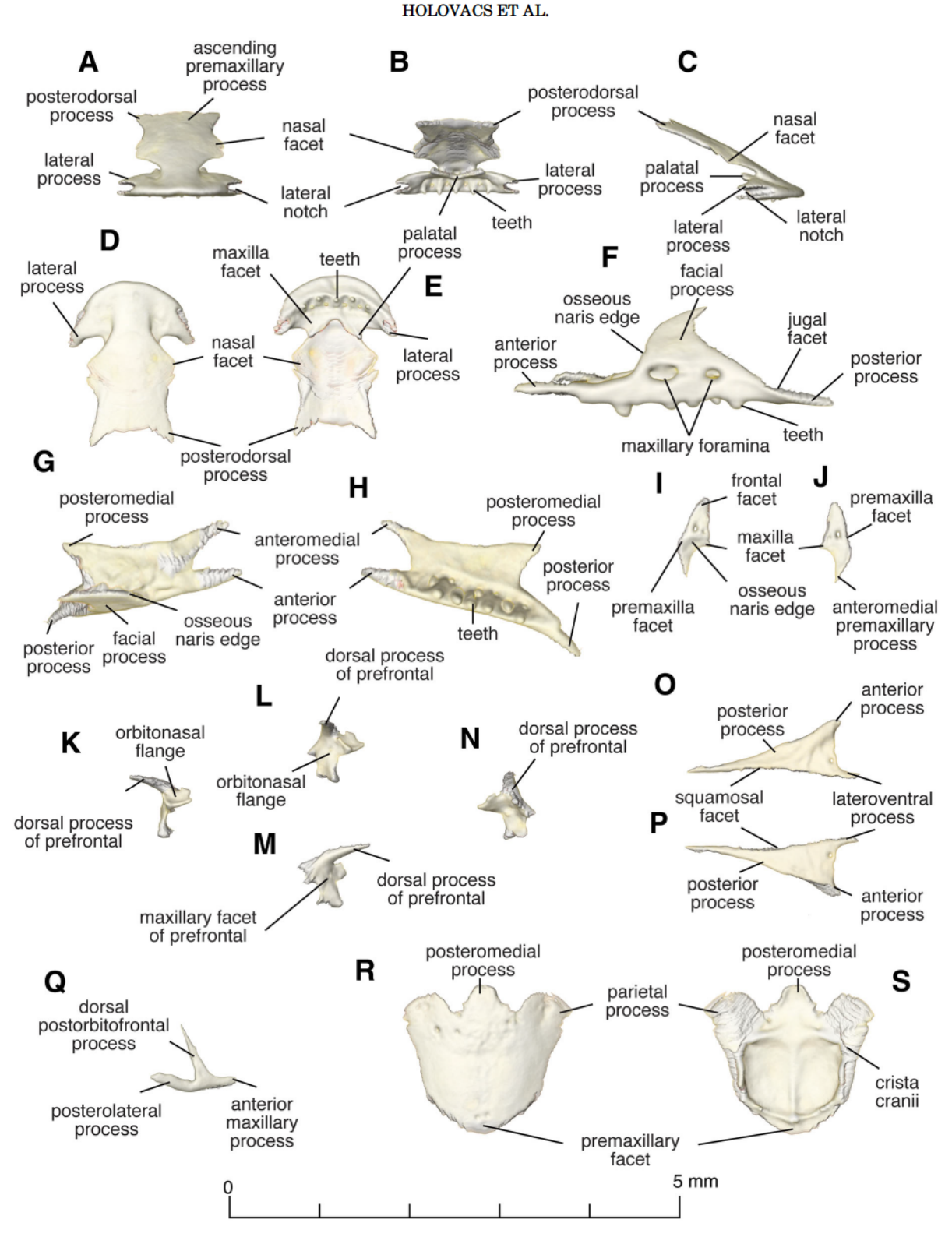


Fig. 6. Individual bone segmentation of Calyptommatus leiolepis (FML 30530). (A-E) premaxilla, (F-H) maxilla, (I, J) nasal, (K-M) prefrontal, (O, P) postorbitofrontal, (Q) jugal, and (R, S) frontal.

Parietal. This bone in C. leiolepis remains unfused in the anterior portion, a residue of the parietal fontanelle in the juvenile specimens; in adults of C. nicterus, the intraparietal suture is completely closed (Figs. 4A and 7A-C). Another difference among these species is the major development of a medial constriction in C. leiolepis, which leaves the prootic portion of the braincase exposed in dorsal view. The significant development

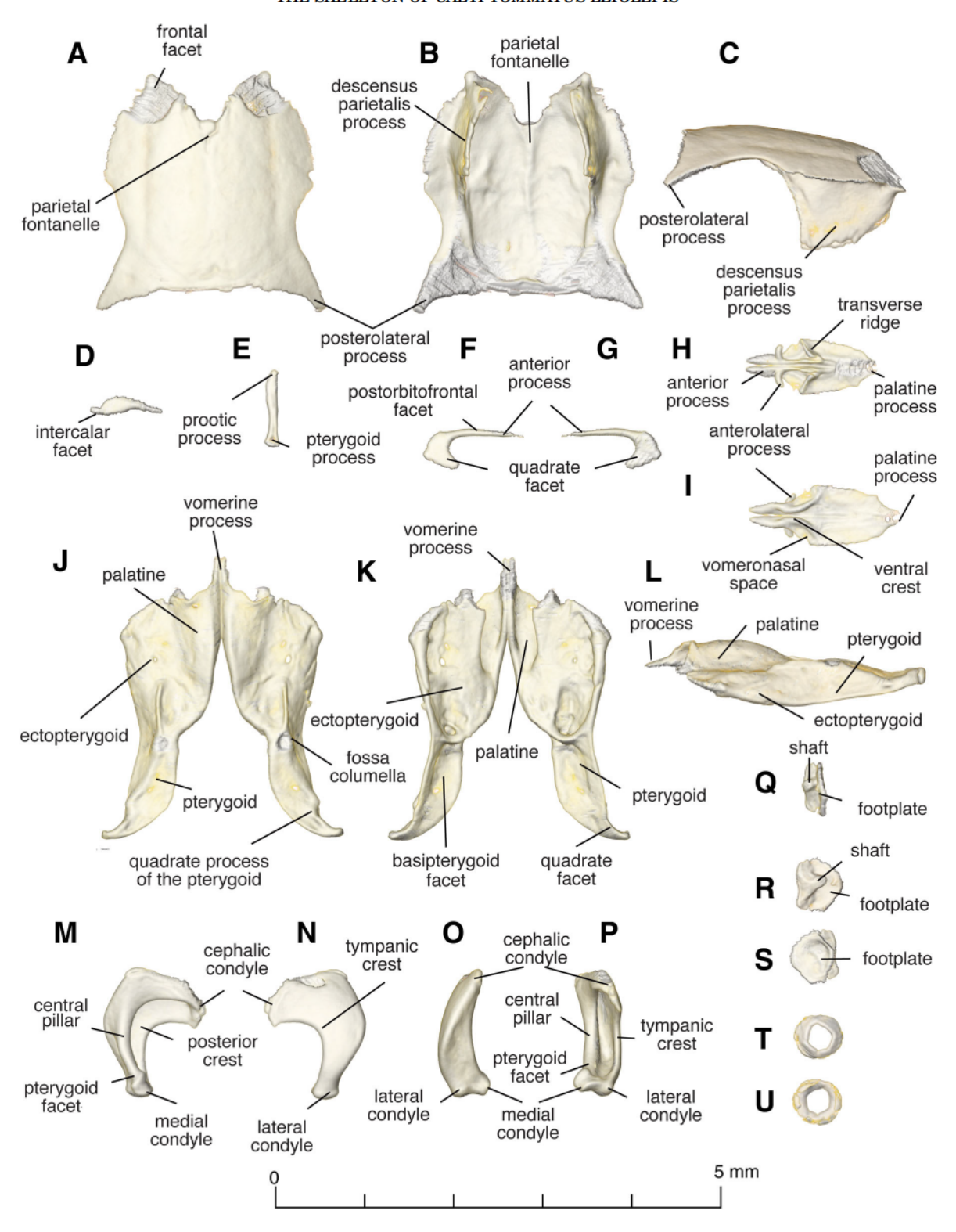


Fig. 7. Individual bone segmentation of Calyptommatus leiolepis (FML 30530). (A-C) parietal, (D) supratemporal, (E) epipterygoid, (F, G) squamosal, (H, I) vomer, (J-L) palatine and pterygoid, (M-P) quadrate, (Q-S) stapes, and (T, U) sclerotic ring.

of a decensus parietalis process in the genus *Calyptommatus* contributes to the anterolateral closure of the braincase and creates a medial walling for the infratemporal recess, together with the epipterygoid and

orbitosphenoids. The decensus parietalis process has a nearly rectangular shape with more or less straight ventral margin and remains separated from the pterygoid, epipterygoid, and orbitosphenoids (Fig. 4A). The frontal

overlaps this bone on the frontal facet, located on the anterior end of the parietal dorsal to the decensus parietalis process (Fig. 7B, C). The posterolateral process is short and ends on a rounded tip; this process is more rounded than in *C. nicterus* (Fig. 4A–C).

Supratemporal. This is a small splint of bone inserted between the postparietal process of the parietal and the squamosal (Figs. 4A and 7D). In *C. leiolepis*, it is in contact with the cephalic condyle of the quadrate or the paroccipital process of the otooccipital posteriorly as in *C. nicterus*, where this bone seems to be more vertically oriented. This orientation positions the dorsal process in between the parietal and the start of the squamosal shaft (Figs. 4A and 7D).

Epipterygoid. This is a columnar bone that lies between the prootic and the decensus parietalis process of the parietal (Fig. 4A). It contributes to the closure of the braincase laterally and is inserted in the fossa columella of the pterygoid. The bone is compressed and bladelike (Figs. 4A and 7E).

Squamosal. The bone has the typical hockey stick shape of lizards (Figs. 4A and 7F, G; Robinson, 1967; Rieppel, 1994). The shaft is curved and has a long overlapping suture with the postorbitofrontal (Fig. 4A). It defines the lateral margin of the supratemporal fenestra (Fig. 4A). The posterior process is lateroventrally expanded and contacts the dorsal surface of the quadrate (Fig. 4A).

Vomer. This bone is elongated in C. leiolepis and is not entirely fused in adults. The paired vomers remain separated anteriorly and posteriorly, in the former producing a posterior expansion for the premaxilla-vomer fenestra and, in the later, an anterior expansion of the interpterygoid vacuity (Figs. 4C and 7H, I). The vomer also forms the posteromedial margin of the fenestra vomeronasalis, the medial margin of the fenestra exochoanalis, and participates in the choana. The anterior processes of the vomer are continued posterolateraly into two conspicuous ventral crests (Fig. 71). In dorsal view, the anterior process shows two short anterolateral processes, which together with two transverse ridges define the area occupied by the vomeronasal organ (Fig. 7H). In the ventral view, the vomer is overlapped by the palatine on the posteriorly located palatine process (Fig. 4C).

Palatine. This bone is nearly rectangular in shape and overlaps the posteromedial portion of vomer and a large triangular area that corresponds to the posteromedial flange of the maxilla (Fig. 4C). Posteriorly, this bone is overlapped by the pterygoid and slightly by the ectopterygoid (Fig. 4C). The palatine is extremely furrowed, forming a duplicipalatinate palate that is partially covered by a cartilaginous sheet that forms an incomplete soft palate. In the HRCT model, the palatine bone was rendered in combination with the pterygoid and ectopterygoid because the resolution of the scan did not allow these bones to be separated; however, in the cleared and stained specimen, it was evident that they are not fused but clumped together (Figs. 4C and 7J-L). The palatine forms the posteromedial border of the small suborbital fenestra (Fig. 4C).

Ectopterygoid. This bone is triangular, flattened, and broad (Fig. 7J–L). It does not contact the maxilla anteriorly but has extensive contact with the maxilla medially and with the pterygoid posteriorly (Fig. 7J–L). In *Calyptommatus*, this bone becomes enlarged, and as a consequence, the suborbital fenestra becomes extremely reduced (Fig. 4C; Roscito and Rodrigues, 2010). This bone forms the posterolateral border of the suborbital fenestra (Fig. 4C).

This is the longest bone of the skull. In Pterygoid. C. leiolepis, it is excluded from the suborbital fenestra by the extensive contact between the palatine and the ectopterygoid (Figs. 4C and 7J-L). The bone bears on its dorsal surface the fossa columella where the epipterygoid inserts (Fig. 7J). The pterygoid participates in the synovial joint with the braincase. Posterior to this articulation, the bone develops two inward blade-like structures that cover ventrally the lateral margins of the braincase (Fig. 4C). Contrary to C. nicterus (Roscito and Rodrigues, 2010), in C. leiolepis, the pterygoid has two discrete anterior processes, a pointed lateral process that bounds the ectopterygoid posteriorly, and a broad and nearly transverse medial process (with a minimal projection) that contacts extensively the palatine (Figs. 4C and 7J-L). In the posterior region of the pterygoid, a laterally pointed quadrate process with a quadrate facet abuts the quadrate for articulation with the jaw (Fig. 4C).

Quadrate. This bone is suspended from the squamosal, supratemporal, and the paroccipital process (Fig. 4A—C). The mandibular articulation is bicondylar: the lateral condyle is slightly larger than the medial one (Fig. 7M—P). The anterior, lateral, and medial surfaces of the quadrate are convex, and the posteroventral surface is slightly concave (Fig. 7M—P). The posterior concavity defines a reduced middle ear space that is mostly filled by the columella auris and some small ossifications. Between the posterior crest and central pillar, there is a large cavity that extends within the body of the quadrate (Fig. 7M, P). On the ventral region, dorsal to the medial condyle, there is a pterygoid facet in which the pterygoid abuts for mandibular articulation (Fig. 7M, P).

Stapes. This bone is highly modified having a rivet shape, consisting of a broad footplate joined by a very short and subtriangular shaft (Fig. 7Q–S). The footplate fits tightly into the fenestra ovalis (Figs. 4A and 8C). Its shaft is very short and is expanded laterally from where a thin and wing-like extrastapes originates (Figs. 4A, 7Q–S, and 8B–C). These two structures combine to form the columella auris.

Sclerotic ring. The ossicles within this ring structure of the orbit are reduced and completely fused creating a cone-like appearance (Figs. 4A, B and 7T, U). Additionally, the sclerotic ring is narrow and steeply angled, as if pointing laterally out of the orbit (Fig. 4A, B). This morphology mirrors all other squamate groups that are also fossorial and have not completely lost the development of the sclerotic ring (Atkins and Franz-Odendaal, 2016).

Neurocranium. In *C. leiolepis*, the sutures are easy to identify. Compared to *C. nicterus*, this species has a more globular braincase (Fig. 8A–F). In general, these two species present similar suturing in the braincase.

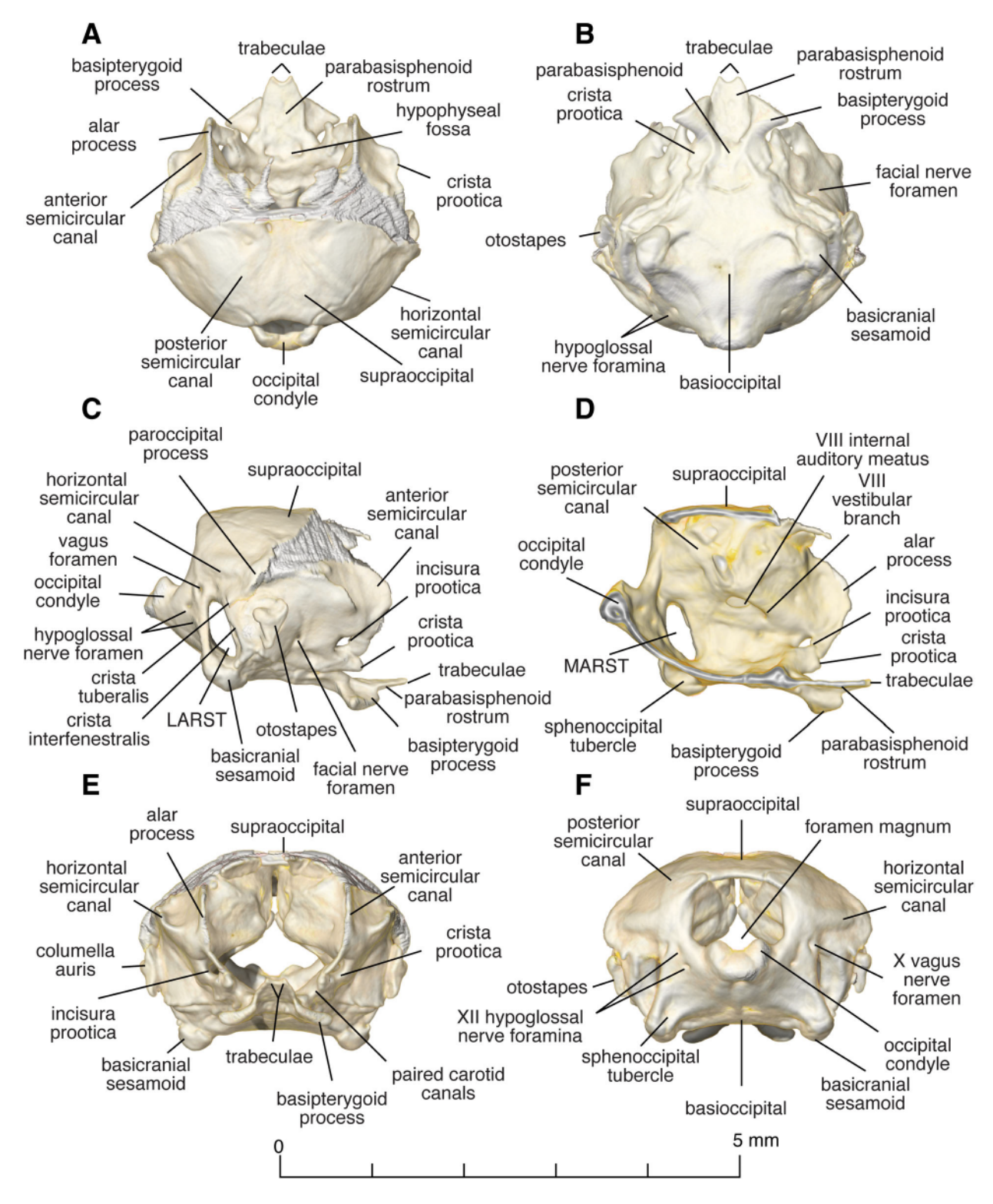


Fig. 8. Braincase (A-F) of Calyptommatus leiolepis (FML 30530).

Orbitosphenoid. The paired orbitosphenoids are small and slender bones that are anteriorly placed in the braincase, just in front of the decensus parietalis process of

the parietal. These two bones are articulated medially in front of the braincase. The resolution made the rendering of these bones difficult.

Prootic. The crista alaris is absent, and this creates a rectangular outline when viewed laterally (Fig. 8C). This anterior part of the basicranium contacts only the epipterygoid, which lies between the braincase and the decensus parietalis process (Fig. 6A). Anterior to the prootic, there is a downward projecting process that includes the incisura protica. In Calyptommatus, the incisura prootica is entirely closed and pierces the prootic. so instead of being a notch, it is a foramen (Fig. 8C-F). The same foramen is developed convergently in nearly all gekkotans and in that group is called the foramen prootico (Daza et al., 2013). Roscito and Rodrigues (2010) described the presence of a crista prootica, but they did not specify in which three burrowing taxa it was present. In Calyptommatus, the crista prootica is poorly developed, and below it, there is a limited space for the recesus vena jugularis, which is partially covered by a medial laminar projection of the pterygoid. The facial foramen opens laterally, posterior to the foramen prootico, and just anterior to the fenestra ovalis (Fig. 8C). The prootic forms the anterior margin of the fenestra ovalis (Fig. 8A-F).

Otooccipital. This bone forms the posterolateral side of the cranium (Figs. 4A, C, and 8A–F). It forms the posterior half of the fenestra ovalis and the anterodorsally oriented fenestra rotunda (which is oval in shape instead of round, Fig. 4A, C). The fenestra rotunda in lizards is also termed the lateral opening of the recessus scalae tympani (LARST; Rieppel, 1985). The LARST in Calyptommatus is located posterior to the fenestra ovalis; this seems to be shared also with Scriptosaura, while in other squamates, LARST is usually located below the fenestra ovalis (Figs. 4A and 8C, D).

The fenestra ovalis and the LARST are separated by the crista interfenestralis, which narrows ventrally and expands dorsally toward the paroccipital process (Fig. 8C). The paroccipital process is very reduced and located dorsally from the stapes (Fig. 8C). The crista tuberalis is very faint, and originates posteriorly, curving around the posterior border of the fenestra rotunda (Fig. 8C). The crista tuberalis projects ventrally toward the ventrally directed sphenoccipital tubercle where it is capped by a distinct ossification, the basicranial sesamoid (Fig. 8B-F, see also Montero et al., 2017). Posterior to the crista tuberalis, there is a well-defined vagus foramen, which marks the division between the two elements that compose the otooccipital, the opisthotic and exoccipital (Fig. 8C; Bever et al., 2005). Below the vagus foramen are two hypoglossal nerve foramina (Figs. 4A and 8B, C, F). In C. nicterus and other gymnophthalmids, two (Bell et al., 2003; Guerra and Montero, 2009; Roscito and Rodrigues, 2010) or three (Tarazona et al., 2008) small foramina have been described. The otooccipital forms the lateral margin for the foramen magnum and they participate in the formation of the prominent occipital condyle (Figs. 2A-C, 4A-C, 5B, 8A-D, F).

Supraoccipital. This bone forms the dorsal margin of the foramen magnum, and its posterior margin is rounded (Figs. 2A, B, 4A, B, 5B, and 8A–F). This bone is completely roofed by the parietal in *C. leiolepis*, and as consequence, the posttemporal fenestrae disappears; the lack of these fenestrae is a difference with *C. nicterus* where two slender openings are persistent (Figs. 4B and 5B). The processus ascendens tectum synoticum in *C. leiolepis* is not

developed; therefore, the parietal and the supraoccipital developed a wide sutural contact (Figs. 2A and 4B).

Parabasisphenoid. This bone presents medially an elongated parabasisphenoid rostrum, from where the cartilaginous cultriformis process originates (Figs. 2C, 4C, and 8A–E). The cultriformis process extends up to the level of the vomer. The parabasisphenoid rostrum extends farther anteriorly than the basipterygoid process (Figs. 2C and 4C). The basipterygoid processes are covered by cartilaginous pads and form a synovial joint with the medial flange of the pterygoid. The basisphenoid is pierced by the abducens canal and the Vidian/carotid canals (Oelrich, 1956; Conrad, 2004; Bever et al., 2005). In the ventral view, the posterior opening of the Vidian canal is visible near the base of the basipterygoid process.

Basioccipital. This bone forms the majority of the occipital condyle (Figs. 2C, 4C, 5B, and 8B, F). The occipital condyle bulges posteriorly, which is a character found in miniaturized species (Figs. 2C, 4C, 5B, and 8B, F, Daza et al., 2009). The occipital condyle is nearly rhomboid and convex ventrally. In the specimens of *C. leiolepis*, we did not find any contribution to the border of the LARST, but it forms the projection of the sphenoccipital tubercles (Fig. 8B–F).

Jaw

Each ramus of the jaw is comprised of six bone elements: the dentary, coronoid, splenial, angular, surangular, and compound bone (Fig. 5C–F). Overall, the posterior portion of the jaw exhibits signs of fusion that obscure the distinct suture lines for individual bones.

The dentary extends posteriorly, coming in contact with the angular ventrally via the superior and inferior processes (Fig. 5C–F). The superior process extends to about the posterior edge of the coronoid, while the inferior process stops at the anterior portion of the external mandibular fenestra (Fig. 5C, F). This bone is concave, curving medially, containing three mental foramina within the anterior one-third of the lateral surface (Fig. 5C). Each dentary contains approximately 10 pleurodont teeth that are well spaced and recurved with somewhat expanded bases (Fig. 5C, D, F). The dentition resembles that of certain groups of Amphisbaenidae, Pygopodidae, Anguidae, Helodermatidae, and Varanidae that contain recurved teeth that come to sharp terminal points (Edmund, 1969).

The splenial contains two foramina that are visible on the medial surface, the alveolar foramen and anterior mylohyoid foramen (Fig. 5F). These foramina are found ventral to the anteromedial process of the coronoid (Fig. 5F).

The angular is small and in a posterior position within the jaw, making contact with the compound bone posteriorly, splenial anteriorly, and surangular dorsally. The posterior mylohyoid foramen is positioned anteroventrally, almost making contact with the surangular posteromedially (Fig. 5E, F). On the lateral face of the surangular, the large surangular foramen comes in contact with the coronoid ventrally, below with the posteromedial process, and is in close contact posteriorly with the posterodorsal process of the dentary (Fig. 5C). The compound bone (prearticular-articular bone) extends posteriorly from the coronoid and dentary (Fig. 5C-F). Between the

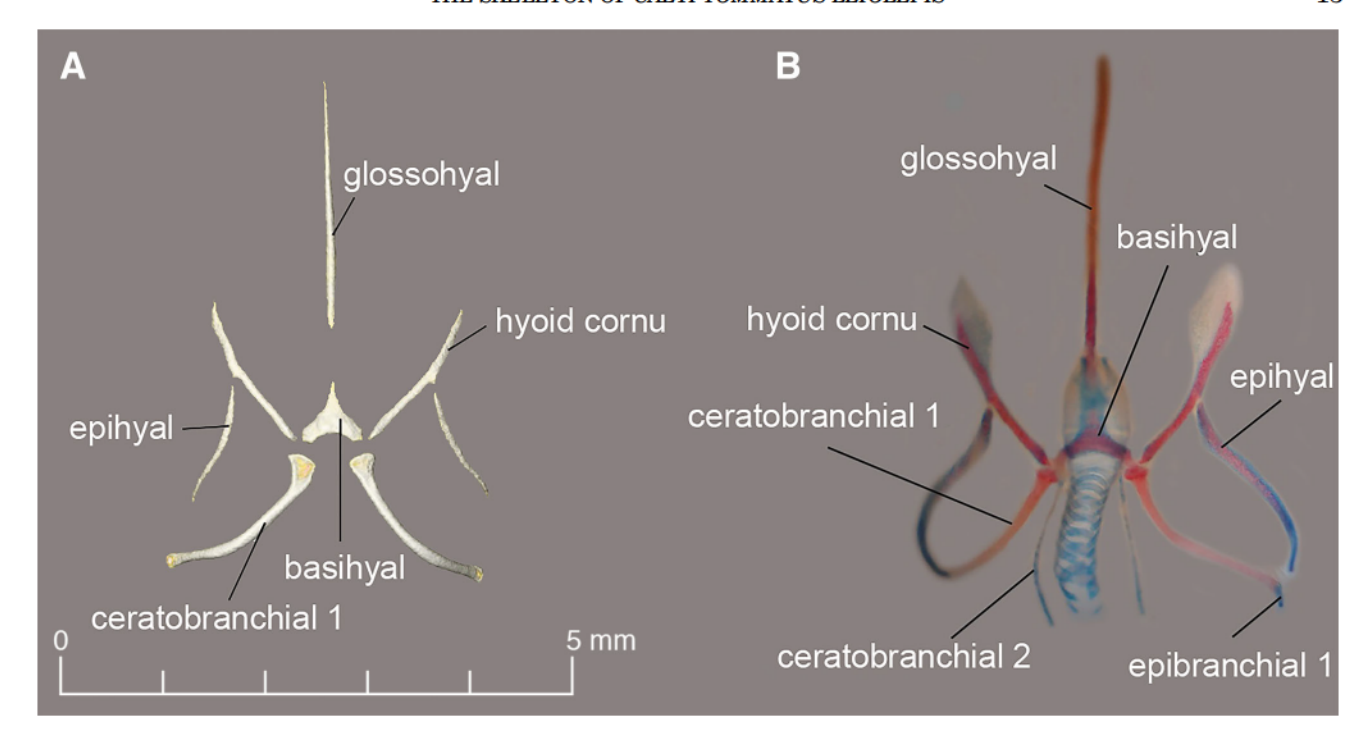


Fig. 9. Hyoid apparatus of Calyptommatus leiolepis (FML 30530) in ventral view. (A) Individual bone segmentation of the osseous elements. (B) Cleared and stained preparation.

retroarticular process and posterior part of the surangular is a concave fossa where the quadrate articulates (Fig. 5D). The articulation occurs in between the lateral and medial condyles of the quadrate.

Hyoid apparatus. The apparatus consists of five ossified/bone elements (three paired and one unpaired) and two cartilaginous elements: basihyal, hyoid cornu, glossohyal, first ceratobranchial, epihyal, first epibranchial, and second ceratobranchial (Fig. 9A, B). The second epibranchial was not found on any of the prepared specimens. The basihyal is shaped like a shark tooth with the apical process pointing toward the mandibular symphysis and the two basal processes extending posterolaterally (Fig. 9A, B). Extending anterolaterally from the lateral position of the basal processes of the basihyal is the hyoid cornu (Fig. 9A, B). This structure extends toward the inferior process of the dentary. The glossohyal is positioned medially and is angled at about 45 degrees toward the vomer (Fig. 9A, B). Positioned posteriorly of the basal processes of the basihyal are the ceratobranchials, of which it articulates. This ossified element extends posterolaterally as well as angles dorsally pointing toward the atlas (Fig. 9A, B). Posterior to the basilyal, there are straight filamentous projections that follow the trachea posteriorly, extending beyond the first ceratobranchial (Fig. 9B). Attached to the first ceratobranchial on the posterolateral end is a small cartilaginous element, the first epibranchial (Fig. 9B).

Pectoral girdle. The pectoral girdle consists of a clavicle, interclavicle, suprascapula, scapulocoracoid, sternum, xiphisternum, and parasternum (Figs. 10A, B and 11). The clavicle is thin and narrow, located anteriorly from the scapulocoracoid and interclavicle (Fig. 10A, B).

The clavicle contacts the suprascapula dorsolaterally and interclavicle posteriorly (Fig. 10A, B). The interclavicle is positioned anteriorly from the sternum following the contour of the two anteromedial sternal processes (Fig. 10A, B). Overall, the pectoral girdle is similar in morphology to that of C. nicterus but is distinct in that it contains a larger (~×4) central foramen within the sternum, a sternum that extends further posteriorly, and a narrower suprascapular (Roscito and Rodrigues, 2012). To increase rigidity to the pectoral region, Calyptommatus leiolepis has developed a consolidation of the rib cage via the parasternum, which consists of a series of ventral bony ribs that overlap the adjacent structures in an analogous way to the uncinate processes of the birds (Fig. 11). The presence of parasternal ribs has also been reported in other gymnophthalmids (e.g., Bachia intermedia, C. nicterus, Nothobachia ablephara, and S. catimbau) and seems to be a synapomorphic trait for some groups within the Gymnophthalmidae (Camp, 1923; Presh, 1975; Roscito and Rodrigues, 2013).

Pelvic girdle and limbs. The pelvic girdle contains a long hypoischium (~2 mm) that extends posteromedially from the pubic tubercle (Fig. 10C). On the posterolateral edge of the girdle between the ischium and pubis, there is a small obturator foramen (Fig. 10C, D). Lateral to the obturator foramen is a small lateral pectineal process that contours the femoral condyle (Fig. 10D). On the posteromedial edge of the ischium there is a poorly developed ischial tuberosity that is directed posterolaterally (Fig. 10D). There is a dorsally directed epiphyseal tuberosity extending from the ilium (Fig. 10E). The pelvic girdle exhibits no fusion on the medial edges of both the ischium and pubis (Fig. 10C, D). The femur is the same length as

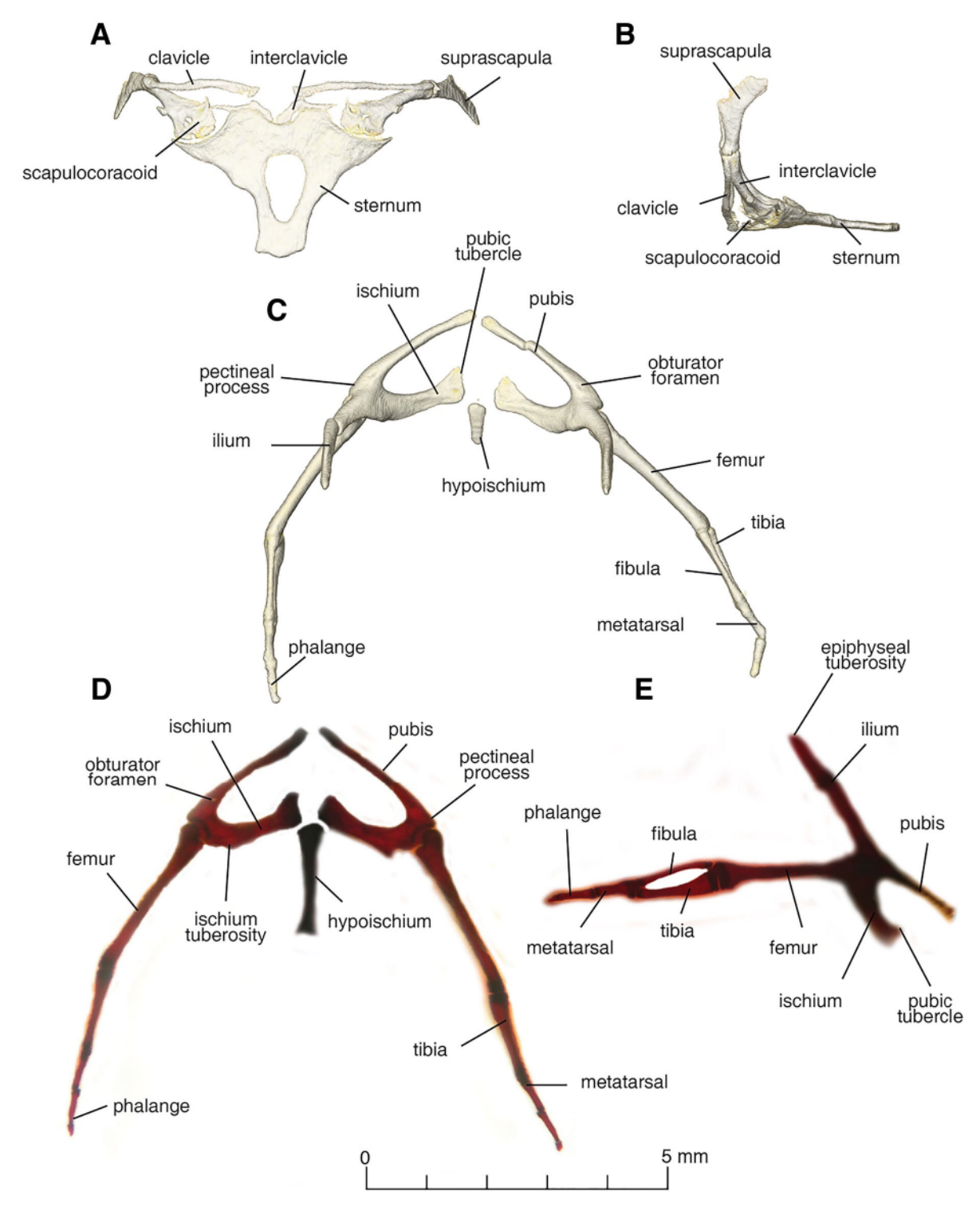


Fig. 10. Pectoral (A, B) and pelvic girdles (C-E) of Calyptommatus leiolepis (FML 30530).

the phalange, metatarsal, fibula, and tibia combined ($\sim 2.75~\text{mm}$) and is directed posterolaterally (Fig. 10C–E). The hind limb exhibits only a single metatarsal and a phalanx that are roughly the same length ($\sim 0.75~\text{mm}$) (Fig. 10C–E).

Cervical vertebrae. The cervical vertebrae exhibit a concave morphology of the neural arches, which are pointed medial at the dorsal tip (Fig. 12A–E). In the middle portion of the neural arches, there is a very small posterodorsal process (Fig. 12A–E). Below the posterodorsal process, on

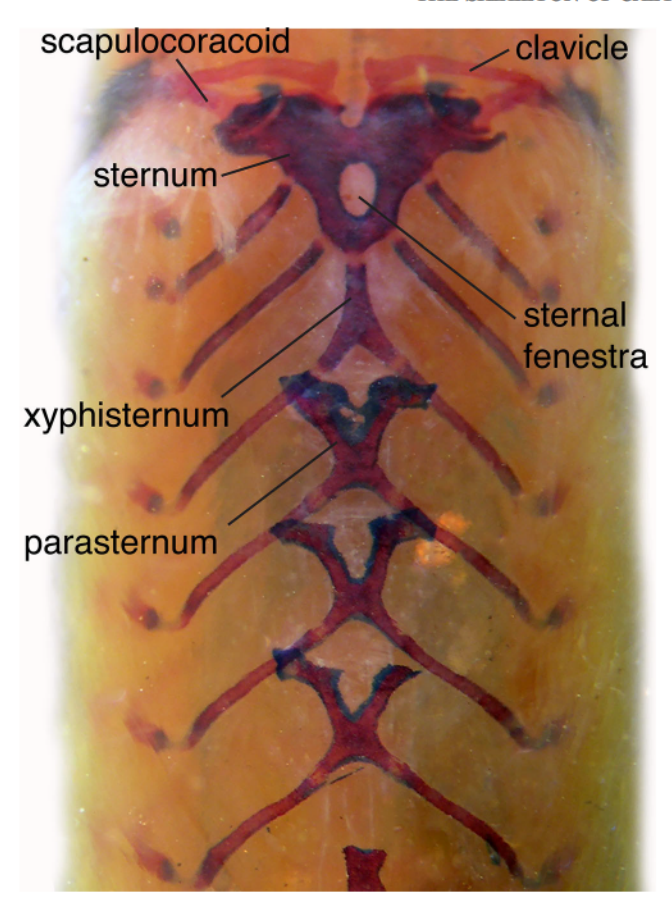


Fig. 11. Pectoral girdle of *Calyptommatus leiolepis* (FML 30530) highlighting the parasternum.

the anterior side of the atlas, there is a small laterally curved transverse process that connects to the cotyle for the occipital condyle (Fig. 12B), which is the point of contact between the atlas and braincase for universal movement of the cranium (Fig. 12B). In the dorsal and lateral views, the vertebrae are tapered at the ventral end and become wider behind the posterodorsal process (Fig. 12D–E). The intercentrum is located on the ventral portion of the vertebrae and exhibits very small contact with both arches, medially from the transverse processes (Fig. 12A–C).

The axis is tall, containing two prominent blade-like processes on the dorsal and ventral surfaces (Fig. 12F). The dorsal neural spine is angled posteriorly with a slight anterior overhang (Fig. 12F). Below the neural spine, there is a small projection of the postzygapophysis that comes in contact with the succeeding vertebra's prezygopaphysis (Fig. 12F). The transverse process is directed posterolaterally and extends past the body of the vertebra (Fig. 12G). There is a large anteriorly projected odontoid process that makes contact with the odontoid process facet of the atlas (Fig. 12A). The odontoid process is wide at the base and tapers to a small anterior process (Fig. 12F, G).

Thoracolumbar vertebrae and ribs. Each of the trunk vertebrae are proceedous and contain a more conspicuous dorsal neural spine, anterodorsally directed prezygopophyses, posteroventrally directed postzygapophyses,

and lateral synapophyses with which the tubercles of the ribs make contact with the vertebra (Fig. 12H-M). The presacral vertebral series varies in neural spine length and direction, length of the centrum, and thickness of the hypapophysis (Fig. 12H-M). The anterior presacral vertebrae, located in the thoracic region above the sternum, are short in centrum length (~1.2 mm) and stout (Fig. 12H). In the lateral view, the neural spine is tall and directed slightly posteriorly (Fig. 12H). On the ventral side of a presacral vertebra, the hypapophysis is thin and directed ventrally slightly passed the synapophysis (Fig. 12H, I). The next posteriorly located presacral vertebra has a blunt neural spine that is directed further posteriorly as well as a more rounded hypapophysis that does not project ventrally passed the synapophysis (Fig. 12J). The next vertebra exhibits the same process of blunting of the hyapophysis and neural spine with an even more posteriorly angled neural spine (Fig. 12L, M).

The ribs contact the vertebrae at the synapophyses and are present in all presacral vertebrae except for the first three cervical vertebrae (Fig. 14). From anterior to posterior, the ribs extend laterally from the vertebral column and reach a maximum width at about the midpoint of the column and then constrict toward the sacrum (Fig. 14).

Sacrum. This bone is formed by the fusion of two sacral vertebrae; these two vertebrae define two sacral foramina, one between each of the connections of the transverse process for each sacrale vertebra (Fig. 13A, B). Both sacrale foramina are located medially within the vertebra ~0.5 mm from the midline (Fig. 13A). This bone also contains two neural spines, the anterior one is shorter in length compared to the posterior one (Fig. 13A, B), which is almost twice as long as the anterior one.

In fully limbed squamates, the sacrum is formed by two vertebrae (Hoffstetter and Gasc, 1969). Deviation from this morphology is common with the incorporation of a vertebra anterior or posterior to the two original sacral vertebrae (Hoffstetter and Gasc, 1969). Within groups of fossorial and limb-reduced squamates, the sacral vertebrae became fused at their neural spine, central, and distal ends of their transverse processes. The fusion of these two vertebrae is not complete, thus leaving a small sacral foramen clearly visible on the ventral side (Fig. 13A). This simplification of sacral morphology within *Calyptommatus leiolepis* can be seen in other groups such as *Bachia*, *Ophiodes*, and others (Camp, 1923; Hoffstetter and Gasc, 1969).

Caudal vertebrae. The caudal vertebrae are elongated (Fig. 12N). The caudal vertebrae have longer neural spines than in the sacral and presacral vertebrae (Fig. 12F-O). On the dorsal tip of the neural spine, there is a slight anteriorly positioned notch (Fig. 12N). Due to the elongated nature of the caudal vertebrae, the intervertebral foramen is slightly extended to the center of the vertebra, giving it a more oval appearance (Fig. 12N). The prezygapophysis is also extended anteriorly 0.5 mm from the chevrons (Fig. 12N). These vertebrae contain two pairs of transverse processes that extend laterally on either side, a unique characteristic of only a few squamate groups (Etheridge, 1967; Fig. 12N, O). On the anterior end of the last caudal vertebra, there seems to be an autotomic septum located just prior to what would be the transverse processes, exhibiting Type 3 location of Etheridge (1967; Fig. 12N, O). Overall, the caudal vertebrae change drastically in morphology from the first vertebra to the last.

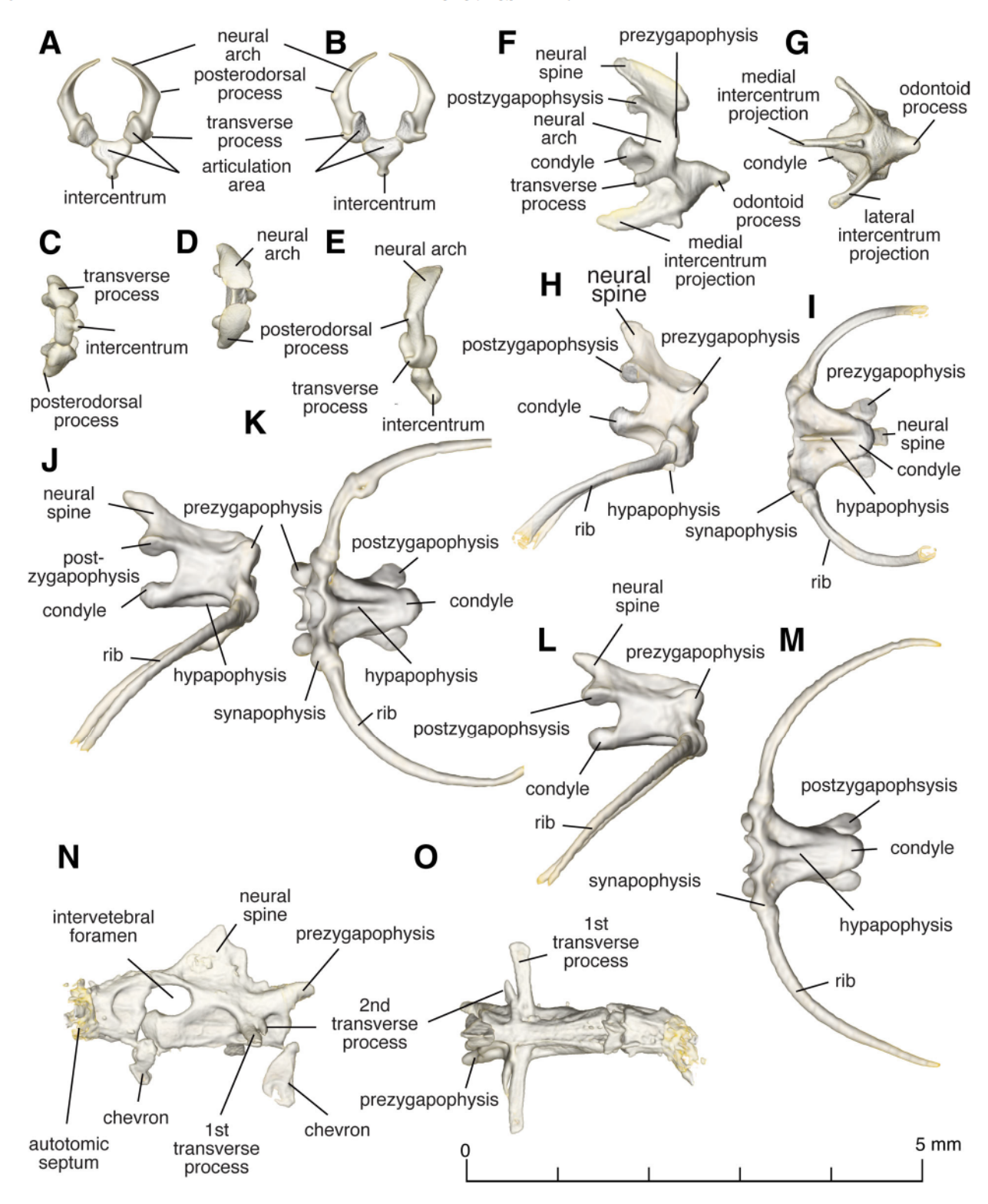


Fig. 12. Vertebrae of Calyptommatus leiolepis (FML 30530), atlas (A-E), axis (F, G), trunk (H-M), and caudal (N, O) vertebrae.

Phylogenetic Analysis

A maximum parsimony analysis was carried out with the morphological data set (Gauthier et al., 2012) of 193 taxa including unordered and ordered coded characters for Calyptommatus leiolepis. The analysis revealed the position of *C. leiolepis* to be nested within the Gymnophthalmidae, although there is no support for Gymnophthalminae (*Colobosaura + Calyptommatus*) (Fig. 15). For simplicity,

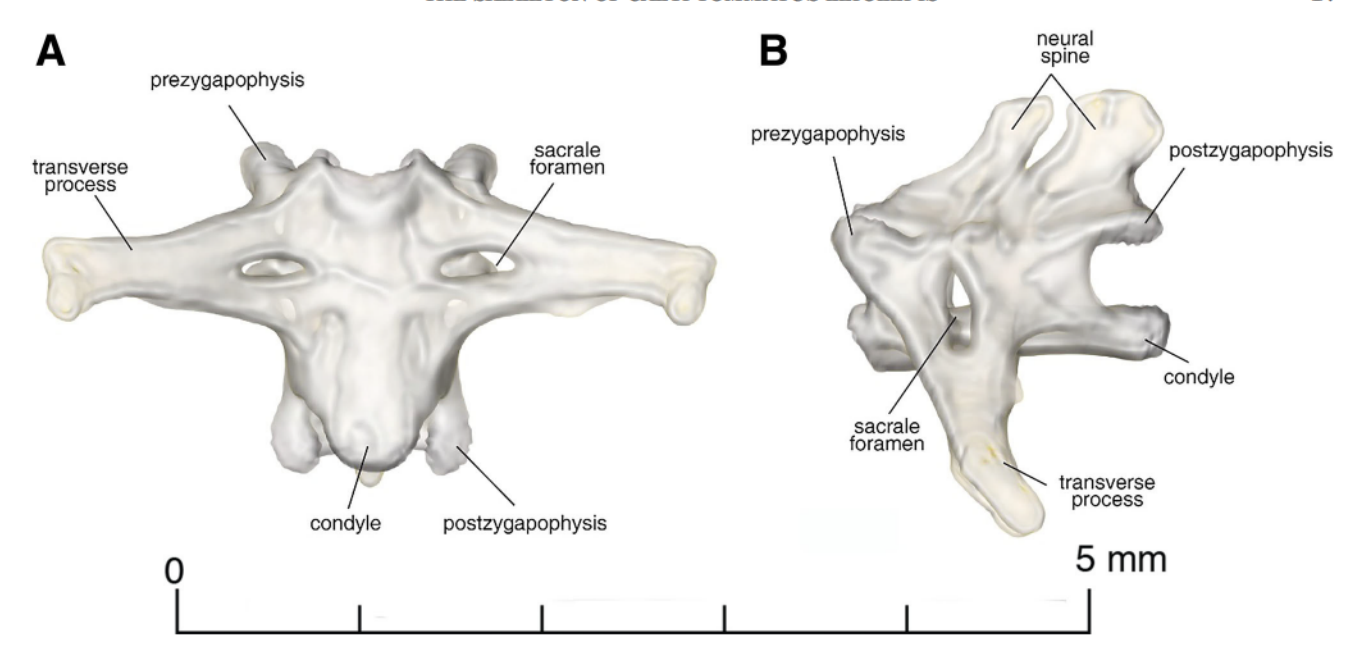


Fig. 13. Sacrum of Calyptommatus leiolepis (FML 30530). A) ventral view, anterior to the top; B) lateral view, anterior to the left.

major clades are collapsed except for taxa within Scincomorpha (Fig. 15). Relationships of major groups (Scincoidea, Teiidae, Gymnophthalmidae, and Lacertidae) were consistent with results from previous analysis using this data set (Gauthier et al., 2012). Synapomorphies that support the placement of Calyptommatus leiolepis within Gymnophthalmidae and are diagnostic for this taxa include characters: 2) premaxilla palatal shelf-(0) not bifid posteriorly; 7) premaxilla body anterior ethmoidal foramina exit via—(1) premaxilla notch; 21) nasal descending lamina— (0) absent; 31) nasofrontal suture shape—(0) without V-shaped nasal process into frontal midline; 65) postfrontal relative to parietal table—(0) ventrolateral; 70) postfrontal broad and flat—(0) not; 81) postorbital-ectopterygoid contact—(0) absent; 82) postorbital jugal ramus— (0) extends ventral to quadrate head; 84) postorbital contribution to posterior orbital margin—(3) 67–8%; 95) parietal postparietal projection near midline—(0) absent; 119) maxilla firmly sutured to palatine—(0) present; 133) prefrontal_frontal suture in cross-section—(0) prefrontal arcs gently about anterolateral frontal margin along entire anteroposterior length; 143) jugal—(0) jugal broadly overlaps level of posterior maxillary tooth row; 166) supratemporal—(0) present; 169) supratemporal anterior

suture with parietal shape—(0) supratemporal lies flat against supratemporal process of parietal; 182) quadratepterygoid overlap—(1) short overlap or small lappet; 185) quadrate height to braincase depth ratio—(1) 50-59%; 190) stapes—(0) imperforate; 191 stapedial shaft—(1) short and thick; 196) septomaxilla—(0) present; 211) vomeronasal organ and mushroom body—(0) not fully enclosed by septomaxilla and vomer; 212) vomer fusion—(1) absent; 258) pterygoid separation on midline—(2) broad at base but not as narrowly separated anteriorly; 308) crista prootica— (0) does not extend onto basipterygoid; 339) basal tubera position—(1) anteromedial with apex at lateral juncture of sphenoid and basioccipital anterior and medial to prooticopisthotic suture; 341) occipital condyle—(0) posterior surface of condyle straight in ventral view; 349) hypoglossal (XII) foramina exit—(0) hypoglossal foramina separated from vagus; 356) dentary anterodorsal edge of dental parapet at tip—(0) straight; 360) dentary subdental shelf/gutter development in anterior part of dentary—(2) pronounced subdental gutter; 361) dentary number of mental foramina on lateral surface—(3) three; 393) coronoid posteromedial process—(1) present; 446) second ceratobranchials—(0) present; 499) clavicle—(0) present; 500) clavicle—(0) no notch or fenestration present; 501) clavicle—(0) rod-like; 503)

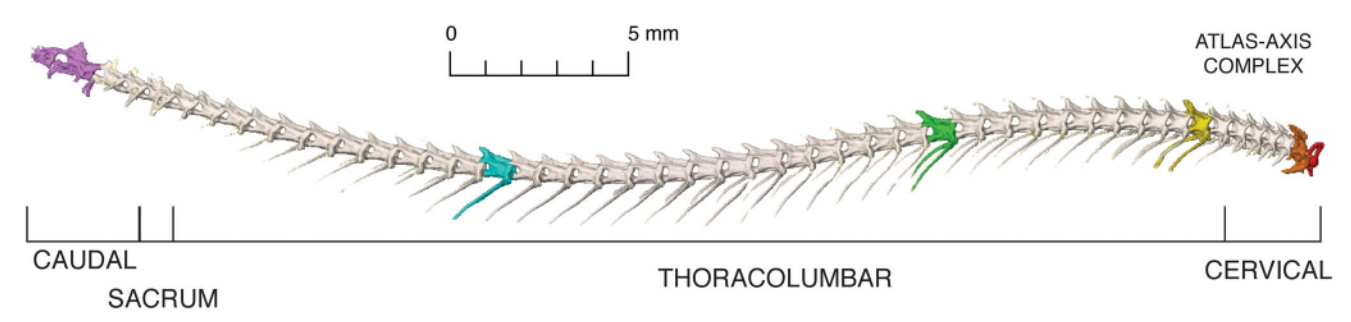


Fig. 14. Vertebral column of Calyptommatus leiolepis (FML 30530). Colored vertebrae are the ones described in detail.

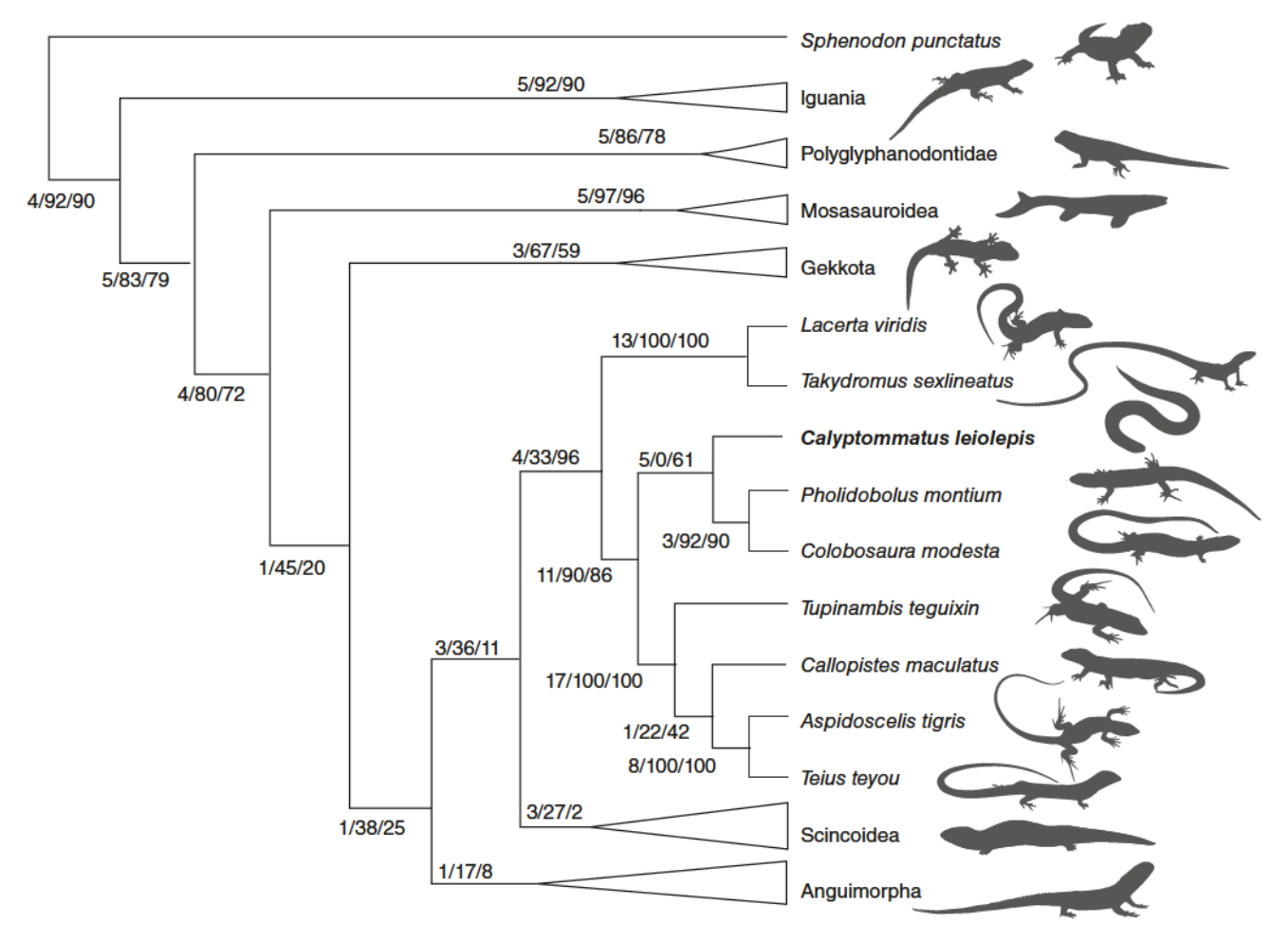


Fig. 15. Phylogenetic position of Calyptommatus leiolepis based on morphological data under the Maximum Parsimony criterion. Support values indicated at each node are Bremer/relative Bremer/bootstrap.

distal clavicle articulation—(1) with suprascapula; 517) ischial tubercle—(0) present; 524) pelvic elements [ilium, ischium, pubis]-(1) distinct elements weakly united in non-sutural contacts; 526) hyperischial foramen-(0) absent; 527) epiphyses on long bones—(1) absent; 548) present; **556**) fibulo-astragalar (0) occupies less than half of distal end of fibula; and 583) mineralized cranial scales hinges—(0) absent. Additionally, the synapomorphies that are diagnostic for gymnophthalmids include: 134) prefrontal length relative to height—(1) short anteroposteriorly; 167) supratemporal shortens—(2) supratemporal very small; 225) vomer posterodorsal margin forms expanded hollow flange-(0) absent; 248) palatine choanal process—(0) forms an extensive concave surface dorsal to the ductus nasopharyngeus: 337) Vidian canal caudal opening—(0) within basisphenoid; 382) angular taller anteriorly closely approaching coronoid-(0) absent; 383) angular medial exposure—(2) narrow; and 460) cervical vertebrae number increase—(0) six or fewer.

DISCUSSION

Calyptommatus leiolepis contains all representative characters of gymnophthalmids: fused frontals, loss of a parietal foramen, and frontal lappets covering the parietal (Estes et al., 1988; Bell et al., 2003). Although these characters are common to gymnophthalmids, there is a large amount of variation within the group and these are also found in Alopoglossidae (Hernández Morales et al., 2019). Much of the variation within gymnophthalmids is found in the temporal and suborbital fenestrae, frontal, parietal, squamosal, palatal elements, presence or absence of lacrimals, postfrontals, postorbitals, tooth counts, and morphology of the jaw and braincase (Bell et al., 2003). Calyptommatus leiolepis comprise many specialized characters that separate it from other taxa within gymnophthalmids as well as other limb-reduced groups. These characters include the head containing a shovel-like snout with a well-developed horizontal keel, nasal cartilages that produce a sand-guard to protect the nostrils. reduced eyes covered by a brille, jugal bone with digit-like posterior projections, lack of forelimbs, extreme reduction of hind limbs, and imbricated scales among others.

Under closer examination using HRCT scan data, the snout of *C. leiolepis* is narrow, but when the whole specimen is visually examined, it appears broad (Fig. 1). This broadening of the snout is due to the specialized development of the rim of connective tissue that expands the

snout width. This is a unique character that no other lizard contains and has allowed *C. leiolepis* to increase the surface area without having to increase bone diameter.

The ocular skeleton of squamates has recently been found to be an important diagnostic character for fossorial squamates (Atkins and Franz-Odendaal, 2016). The ocular skeleton comprises a combination of scleral cartilage and ossicles (Walls, 1942). The presence or absence of these elements is variable among vertebrate groups and are thought to be influenced by behavior (Atkins and Franz-Odendaal, 2016). Groups that have a fossorial lifestyle and are scotopic, contain scleral ossicles that are reduced or absent (e.g., amphisbaenians), while those that are non-fossorial and photopic have well-developed sclerotic rings (Franz-Odendaal, 2008). For C. leiolepis, individual scleral ossicles (~ 14) are present during early stages of development, but these elements become fused in the adult (Roscito and Rodrigues, 2012). Given the tendency of these lizards to burrow within sandy substrates, it is expected that they would correspond more with fossorial and scotopic animals, but this trait has not been observed in C. leiolepis or in the sandswimmer African Sandfish (e.g., Scincus scincus), which has a similar ocular skeleton to C. leiolepis (i.e., fused elements). Additionally, there is a complete external brille covering the eve. This trait is found in many groups of squamates including members of the Pygopodidae, Gekkonidae, Phyllodactylidae, Scincidae, Sphaerodactylidae, Serpentes, and Gymnophthalmidae (Guerra-Fuentes et al., 2014).

The suborbital fenestra is almost lost within *C. leiolepis*. This finding is unusual because the skeletal autapomorphy of having a suborbital fenestra is contained within all basal lineages of diapsids (Evans, 1988). This character is usually made by the bone-to-bone contact between the palatine, ectopterygoid, and the maxilla. This characteristic of closing of the suborbital fenestra is even further exacerbated by a complete closure of the fenestra in *C. nicterus* (Roscito and Rodrigues, 2010).

Another finding includes that of the basicranial sesamoid, which is an ossified element that covers the sphenoccipital tubercle of the basicranium (Fig. 7). In C. leiolepis, the element is large ($\sim 1 \text{ mm}$) and globularshaped. Many other vertebrate groups contain sesamoids, but these elements vary dramatically in shape and size depending on the taxa's degree of fossoriality (Montero et al., 2017). Within squamates, basicranial sesamoids have been found in many families, but in non-fossorial species, the basicranial sesamoid is usually small (Montero et al., 2017). Calyptommatus leiolepis contains a proportionally large basicranial sesamoid (~1 mm) compared to other non-fossorial taxa (Montero et al., 2017). This morphological adaptation toward a larger basicranial sesamoid may be attributed to assisting some of the head movement muscles during burrowing through the substrate. It has been shown that these basicranial sesamoids are anchors of attachment for the longus colli muscle (Montero et al., 2017). The function of this muscle is for movement of the head in a ventral motion. Thus, a larger basicranial sesamoid would increase the surface area for attachment of the longus colli muscle for a greater force for burrowing.

The jugal is another diagnostic character for *Calyptommatus*, containing a tri-radiated morphology. Upon close examination, the posterolateral process is elongated with finger-like projections. This elongation of the posterolateral process of the jugal has been found in other squamate groups, being attributed to the regain of the posttemporal bar (Mo et al., 2009).

Postorbitofrontal is a name that has been applied to the unique element on the posterodosal portion of the orbit in Calvptommatus, a similar situation occurs in some iguanians, all gekkotans and anguids (Camp, 1923; Conrad, 2008; Daza and Bauer, 2010). In squamates, usually the bone that participates in the postorbital bar and the upper temporal bar is the postorbital, while the postfrontal usually clasps the frontoparietal suture (Evans, 2008). Developmental data for gekkotans have shown that in Eublepharis macularius, the postorbitofrontal corresponds only to the postfrontal, but this interpretation is conditioned to an anterior shift of the postorbital to a parafrontal position and its successive fusion with the frontal bone (Wise and Russell, 2010). In Calyptommatus, the postorbitofrontal is indeed formed by the fusion of a well-developed postorbital and reduced postfrontal (Roscito and Rodrigues, 2010).

Although *C. leiolepis* was described as lacking an external ear, it actually does contain a small opening visible in ventral view at the height of the bottom half of the fifth infralabial (Rodrigues, 1991). This opening is also seen in the lateral view where a small tympanic membrane is visible, bounded by the posterior-most upper labials and below the second row of temporal scales. This ear opening is half the diameter of the eye. The presence of a tympanic membrane and the greater modification of the stapes suggest that this animal can perceive low-frequency sounds and possible underground vibrations.

In extremely miniaturized lizards, the size of the foramina is commonly enlarged, seemingly the nerves and arteries that pierce them have to keep a minimum size after a certain point. For instance, the maxillary foramina in *Calyptommatus* are bigger than the foramina in larger species (e.g., *Neusticurus ecpleopus*; Bell et al., 2003).

Inherently, squamates encompass a very large diversity of body forms that range from fully tetrapod to the elongated limbless forms seen in snakes (Bradley et al., 2008; Vitt and Caldwell, 2014). This transition from having four fully developed limbs to a limbless form has been attributed to the modification of vertebral number as well as pectoral and pelvic girdle adaptations (Roscito and Rodrigues, 2013). Taxa that comprise a snake-like body form include not just burrowing taxa but surface and grass dwellers as well (Camp, 1923). The shift toward elongation of the trunk region is thought to have occurred due to the advantageous nature of undulatory locomotion, where movement through dense substrate would be hindered by fully developed limbs (Gans, 1974).

The pectoral and pelvic girdle is directly affected by the shift to a snake-like body form and comprises two patterns of reduction. The girdles can exhibit a greater reduction in the forelimb than the hind limb or have a greater reduction in the hind limb compared to the forelimb (Roscito and Rodrigues, 2013). For example, pygopodids contain taxa that range from terrestrial and fossorial with varying degrees of girdle development (Greer, 1989). Terrestrial taxa contain well-developed pectoral and pelvic girdles, in which the pelvic girdle becomes fused in the adult stage (Stephenson, 1962). Fossorial taxa, on the other hand, have very reduced pelvic and pectoral girdle development, containing unfused pelvic elements (Stephenson, 1962; Greer, 1989). This also occurs within the families Scincidae and Gymnophthalmidae, where there are groups that contain well-developed girdle elements, but those that are fossorial are typically elongated with reduced girdle development (Greer, 1970). For C. leiolepis, the pelvic and

pectoral girdles are very reduced, having unfused puboischiadic halves, reduction in the size of pelvis (~ 4 mm), and reduction of the prehensile elements in the hind limb into one metatarsal and one phalange. These morphological adaptations are also characteristic in other burrowing taxa closely related to this taxon, such as $S.\ catimbau$ and $C.\ nicterus$ (Roscito and Rodrigues, 2013).

Ancestral trunk vertebrae number is 25 (Sphenodon punctatus; Bergmann and Irschick, 2012). Lizard-like gymnophthalmids and some teiids have 25–26 trunk vertebrae, while snake-like species have an increased number of trunk vertebrae (Daza et al., 2018). Specifically, the vertebral column of C. leiolepis consists of 44 presacral vertebrae (Fig. 15). Two modes of elongation have been determined: lengthening of the tail or of the trunk (Wiens and Slingluff, 2001; Wiens et al., 2006). The increased maneuverability of undulatory locomotion through the loose sand habitat in which C. leiolepis dwells resulted on the lengthening of the trunk and acquiring an intermediate sized tail, not being reduced as in "short-tailed burrowers" and not as long as the ones of grass swimming lizards (e.g., Chamaesaura).

The serpentiform body among squamates has been identified as the cause of a long-standing problem in squamate phylogeny, causing major discrepancies in relationships among the major clades (i.e., Gekkota, Iguania, Scincomorpha, Anguimorpha, and Ophidia) based on morphology and molecular data (Losos et al., 2012). One main criticism to morphological data sets is that due to their shared missing appendicular elements, all the limbreduced groups/body-elongated groups are clumped together in a "fossorial group" (Conrad, 2008; Gauthier et al., 2012). One of the main goals of this study was to determine if the morphology of a very derived squamate still supports its placement within the gymnophthalmid lizards or if this taxon would be lumped together with the so-called "fossorial group" identified by Gauthier et al. (2012) that includes dibamids, amphisbaenians, and snakes but excludes limbless pygopods and Anguis. Our results clearly demonstrate that not all fossorial and semifossorial taxa are affected and grouped together with limbless forms (other exceptions are pygopods geckos and the anguimorph Ophisaurus). Calyptommatus leiolepis has a unique combination of derived characters that are diagnostic for this taxon (e.g., shovel-like snout with a welldeveloped horizontal keel, nasal cartilages, reduced eyes covered by a brille, lack of forelimbs, reduction of hind limbs, and imbricated scales), but at the same time, this taxon still retains synapomorphies of gymnophthalmids. Calyptommatus leiolepis has also developed adaptations for semi-fossorial dwelling, but these adaptations differ considerably with other fossorial groups. To some extent, C. leiolepis has reinvented its morphological blueprint to be compatible with its semi-fossorial lifestyle. This can be witnessed by comparing the way that the braincase becomes closed; in the majority of fossorial squamates groups, the parietal and the prootic form the main lateral walls of the braincase—in C. leiolepis, the decensus parietalis process of the parietal is hypertrophied, creating a robust structure for lateral protection and fulfilling the protective function of the brain.

The genus *Calyptommatus* shows very unique morphological traits that are suitable for its sand-swimming locomotion. The adaptations of these lizards represent their habitat and behavior well. This is a rare situation among

squamates, where frequently their morphology is very generalized, and establishing a relationship between ecology and morphology is very difficult (Tulli et al., 2016). In a recent morphometric multivariate analyses (mean snoutvent length, average length of unbroken tail, cubic root of body weight in grams, head length, head width, head depth, foreleg length, and hind leg length) and ecological variables (habitat, diet, life history, metabolism, defense) were used to produce a lizard niche hypervolume (Pianka et al., 2017). Although several gymnophthalmoideans were included in this multivariate analysis (Alopoglossus, Bachia, Arthrosaura, Leposoma, Potamites, and Cercosaura), the genus Calyptommatus was not included; we predict that due to the peculiar morphology and ecology of these limbreduced lizards, they will occupy an undescribed position in the lizard multidimensional space.

ACKNOWLEDGMENTS

This article is the Master of Science Thesis of the senior author (N.T.H.). The senior author thanks the members of its thesis Committee: Juan Diego Daza, Monte L. Thies, and Sibyl R. Bucheli, for their support and help. N.T.H. also thank Sam Houston State University for providing a Teaching Assistantship through its academic career. We thank Dr. Virginia Abdala and Dr. Paulo Vanzolini for access to specimens under they care. Juliana Roscito, Cristian Hernández Morales, and Alexandra Herrera provided commentaries that improve the quality of this article. N.T.H. wants to thank specially to Lauren M. Sommer for her unconditional support through the period of graduate school.

LITERATURE CITED

Arnold EN. 1998. Cranial kinesis in lizards: variations, uses, and origins. In: Hecht M, Macintyre R, Clegg M, editors. Evolutionary Biology, volume 30. New York: Plenum Press. p 323-357.

Atkins JB, Franz-Odendaal TA. 2016. The sclerotic ring of squamates; an evo-devo-eco perspective. J Anat 4:503-513.

Bell CJ, Evans SE, Maisano JA. 2003. The skull of the gymnophthalmid lizard Neusticurus ecpleopus (Reptilia: Squamata). Zool J Linn Soc 103:283–304.

Bergmann PJ, Irschick DJ. 2012. Vertebral evolution and the diversification of squamate reptiles. Evolution 66:1044–1058. https://doi.org/10.1111/j.1558-5646.2011.01491.x

Bever GS, Bell CJ, Maisano JA. 2005. The ossified braincase and cephalic osteoderms of *Shinisaurus crocodilurus* (Squamata, Shinisauridae). Palaeontol Electron 8:1–36.

Bradley MC, Huelsenbeck JP, Wiens JJ. 2008. Rates and patterns in the evolution of snake-like body form in squamate reptiles: evidence for repeated re-evolution of lost digits and long-term persistence of intermediate body forms. Evolution 62:2042–2064.

Camp CL. 1923. Classification of the lizards. Bull Am Mus Nat Hist 48:289–307.

Conrad JL. 2004. Skull, mandible, and hyoid of Shinisaurus crocodilurus Ahl (Squamata: Anguimorpha). Zool J Linn Soc 141:399–434.

Conrad JL. 2008. Phylogeny and systematics of Squamata (Reptilia) based on morphology. Bull Am Mus Nat Hist 310:1–182.

Daza JD, Bauer AM. 2010. The circumorbital bones of the Gekkota (Reptilia: Squamata). Anat Rec 293:402–413.

(Reptilia: Squamata). Anat Rec 293:402–413.

Daza JD, Herrera A, Thomas R, Claudio H. 2009. Are you what you eat? A geometric morphometric analysis of gekkotan skull shape.

Biol J Linn Soc 97:677-707.

Daza JD, Bauer AM, Snively E. 2013. Gobekko cretacicus (Reptilia: Squamata) and its bearing on the interpretation of gekkotan affinities. Zool J Linn Soc 167:430–448.

- Daza JD, Bauer AM, Stanley EL, Bolet A, Dickson B, Losos JB. 2018. An enigmatic miniaturized and attenuate whole lizard from the mid-cretaceous amber of Myanmar. Breviora 563:1–18.
- Edmund AG. 1969. Dentition. In: Gans C, Bellairs A'A, Parsons TS, editors. Biology of the reptilia, morphology A, Vol. 1. New York: Academic Press. p 117–200.
- Estes R, de Queiroz K, Gauthier J. 1988. Phylogenetic relationships within Squamata. In: Estes R, Pregill G, editors. Phylogenetic relationships of the lizard families. Essays commemorating Charles L. Camp. Stanford: Stanford University Press. p 119–281.
- Etheridge R. 1967. Lizard caudal vertebrae. Copeia 4:699-721.
- Evans SE. 1988. The early history and relationships of the Diapsida. In: Benton MJ, editor. The phylogeny and classification of the tetrapods. Oxford: Clarendon Press. p 221–260.
- Evans SE. 2008. The skull of lizards and tuatara. In: Gans C, Gaunt AS, Adler K, editors. Biology of the reptilia, morphology H, Vol. 20. Society for the Study of Amphibians and Reptiles: Ithaca. p 1–347.
- Franz-Odendaal TA. 2008. Toward understanding the development of scleral ossicles in the chicken, *Gallus gallus*. Dev Dyn 237: 3240–3251.
- Gans C. 1974. Biomechanics: an approach to vertebrate biology. Ann Arbor: University of Michigan Press.
- Gans C. 1975. Tetrapod limblessness: evolution and functional corollaries. Am Zool 15:455–467.
- Gauthier JA, Kearney M, Maisano JA, Rieppel O, Behlke ADB. 2012. Assembling the squamate tree of life: Perspectives from the phenotype and the fossil record. Bull Peabody Mus Nat Hist 53:3–308.
- Goicoechea N, Frost DR, De la Riva I, Pellegrino KCM, Sites J, Rodrigues MT, Padial JM. 2016. Molecular systematics of teioid lizards (Teioidea: Gymnophthalmoidea: squamata) based on the analysis of 48 loci under tree-alignment and similarity-alignment. Cladistics 32:1-48.
- Goloboff PA, Catalano SA. 2016. TNT version 1.5, including a full implementation of phylogenetic morphometrics. Cladistics 32: 221-238.
- Greene HW, Cundall D. 2000. Limbless tetrapods and snakes with legs. Science 287:1939–1941.
- Greer AE. 1970. A subfamilial classification of scincid lizards. Bull Mus Comp Zool 139:151–184.
- Greer AE. 1989. The biology and evolution of Australian lizards. Chipping Norton: Surrey Beatty and Sons.
- Greer AE. 1991. Limb reduction in squamates: identification of the lineages and discussion of the trends. J Herpetol 25:166–173.
- Guerra C, Montero R. 2009. The skull of Vanzosaura rubricauda (Squamata: Gymnophthalmidae). Acta Zool 90:359–371.
- Guerra-Fuentes RA, Roscito JG, Nunes PM, Oliveira-Bastos PR, Antoniazzi MM, Jared C, Rodrigues MT. 2014. Through the looking glass: the spectacle in gymnophthalmid lizards. Anat Rec 297:496–504.
- Hernández Morales C, Peloso PLV, Bolívar García W, Daza JD. 2019. Skull morphology of the lizard *Ptychoglossus vallensis* (Squamata: Alopoglossidae) with comments on the variation within Gymnophthalmoidea. Anat Rec 302:1074–1092. https://doi.org/10. 1002/ar.24038.
- Hoffstetter R, Gasc JP. 1969. Vertebrae and ribs of modern reptiles. In: Gans C, Bellairs A, Parsons TS, editors. Biology of the reptilia, volume 1, Morphology A. New York: Academic Press. p 1–373.
- Jerez A, Mangione S, Abdala V. 2010. Occurrence and distribution of sesamoid bones in squamates: a comparative approach. Acta Zool 91:295–305.
- Kearney M, Stuart BL. 2004. Repeated evolution of limblessness and digging heads in worm lizards revealed by DNA from old bones. Proc Royal Soc London 271:1677–1683.
- Lakjer T. 1927. Studien über die Gaumenregion bei Sauriern im Vergleich mit Anamniern und primitiven Sauropsiden. Zool Jahr Abt Anat Ont Tiere 49:57–356.
- Lambertz M. 2010. Kommentierte Liste der squamaten Reptilien des Sanddünengebietes am mittleren Rio São Francisco (Bahia, Brasilien) unter besonderer Berücksichtigung endemischer Faunenelemente. Ophidia 4:2–17.
- Lee MSY. 1998. Convergent evolution and character correlation in burrowing reptiles: towards a resolution of squamate relationships. Biol J Linn Soc 65:369–453.

- Losos JB, Hillis DM, Greene HW. 2012. Who Speaks with a forked tongue? Science 338:1428–1429.
- Maddison, WP, Maddison DR. 2018. Mesquite: a modular system for evolutionary analysis. Version 3.51 http://www.mesquiteproject.org Maisano JA. 2008. A protocol for clear and double-staining squamate specimens. Herpetol Rev 39:52–54.
- Mo JY, Xu X, Evans SE. 2009. The evolution of the lepidosaurian lower temporal bar: new perspectives from the late cretaceous of South China. Proc Royal Soc London 277:331–336.
- Montero R, Daza JD, Bauer AM, Abdala V. 2017. How common are cranial sesamoids among squamates? J Morphol 278:1400–1411.
- Müller J, Hipsley CA, Head JJ, Kardjilov N, Hilger A, Wuttke M, Reisz RR. 2011. Eocene lizard from Germany reveals amphisbaenian origins. Nature 473:364–367.
- Oelrich TM. 1956. The anatomy of the head of Ctenosaura pectinata (Iguanidae). Univ Michigan Mus Zool Misc Pub 94:1–122.
- Pellegrino KCM, Rodrigues MT, Yonenaga-Yassuda Y, Sites JW. 2001. A molecular perspective on the evolution of microteiid lizards (Squamata, Gymnophthalmidae), and a new classification for the family. Biol J Linn Soc 74:315–338.
- Pianka ER, Vitt LJ, Pelegrin N, Fitzgerald DB, Winemiller KO. 2017. Toward a periodic table of niches, or exploring the lizard niche hypervolume. Am Nat 190:601-616.
- Presh W. 1975. The evolution of limb reduction in the teiid lizard genus Bachia. Bull South Calif Acad Sci 74:113–121.
- Pyron RA, Burbrink FT, Wiens JJ. 2013. A phylogeny and revised classification of Squamata, including 4161 species of lizards and snakes. BMC Evol Biol 13:93.
- Rieppel O. 1984a. Miniaturization of the lizard skull: Its functional and evolutionary implications. In: Ferguson MWJ, editor. The structure, development and evolution of reptiles. Symp. Zool. Soc. London, New York: Oxford University Press. 52:503-520.
- Rieppel O. 1984b. The structure of the skull and jaw adductor musculature of the Gekkota, with comments on the phylogenetic relationships of the Xantusiidae (Reptilia: Lacertilia). Zool J Linn Soc 82:291–318.
- Rieppel O. 1985. The recessus scalae tympani and its bearing on the classification of reptiles. J Herpetol 19:373–384.
- Rieppel O. 1994. The Lepidosauromorpha: an overview with special emphasis on the Squamata. In: Fraser NC, Sues H-D, editors. In the shadow of the dinosaurs: early mesozoic tetrapods. New York: Cambridge University Press. p 23-37.
- Rieppel O, Gauthier J, Maisano JA. 2008. Comparative morphology of the dermal palate in squamate reptiles, with comments of phylogenetic implications. Zool J Linn Soc 152:131–152.
- Robinson PL. 1967. The evolution of the Lacertilia. Coll Int Cent Nat Réch Sci 163:395–407.
- Rodrigues MT. 1991. Herpetofauna das dunas interiores do Rio São Francisco, Bahia, Brasil. I. Introdução à área e descrição de um novo gênero de microteiideos (Calyptommatus) com notas sobre sua ecologia, distribuição e especiação (Sauria, Teiidae). Pap Avulsos Zool 37:285–320.
- Roscito JG, Rodrigues MT. 2010. Comparative cranial osteology of fossorial lizards from the tribe Gymnophthalmini (Squamata, Gymnophthalmidae). J Morphol 271:1352–1365.
- Roscito JG, Rodrigues MT. 2012. Embryonic development of the fossorial gymnophthalmid lizards Nothobachia ablephara and Calyptommatus sinebrachiatus. Fortschr Zool 115:302–318.
- Roscito JG, Rodrigues MT. 2013. A Comparative analysis of the postcranial skeleton of fossorial and non-fossorial gymnophthalmid lizards. J Morphol 274:845–858.
- Roscito JG, Nunes PMS, Rodrigues MT. 2014. Digit evolution in gymnophthalmid lizards. Int J Dev Biol 58:895–908.
- Sanger TJ, Gibson-Brown JJ. 2004. The developmental bases of limb reduction and body elongation in squamates. Evolution 58:2103–2106.
- Siedchlag AC, Benozzati ML, Passoni JC, Rodrigues MT. 2010. Genetic structure, phylogeny, and biogeography of brazilian eyelidless lizards of genera Calyptommatus and Nothobachia (Squamata, Gymnophthalmidae) as inferred from mitochondrial DNA sequences. Mol Phyl Evol 56:622–630.
- Stephenson NG. 1962. The comparative morphology of the head skeleton, girdles and hind limbs in the Pygopodidae. J Linn Soc Zool 44:627-644.

- Tarazona OA, Fabrezi M, Ramírez-Pinilla MP. 2008. Cranial morphology of *Bachia bicolor* (Squamata: Gymnophtalmidae) and its postnatal development. Zool J Linn Soc 152:775–792.
- Tulli MJ, Cruz FB, Kohlsdor T, Abdala V. 2016. When a general morphology allows many habitat uses. Integr Zool 11:473–489.
- Uetz P, Hošek J, Hallermann J. 2019. The reptile database. Available at http://www.reptiledatabase.org (Accessed May 7, 2019).
- Vitt LJ, Caldwell JP. 2014. Herpetology, fourth edition: An introductory biology of amphibians and reptiles. London: Academic Press.
- Walls GL. 1942. The vertebrate eye and its adaptive radiation. Oxford: Cranbrook Institute of Science.
- Wiens JJ. 2004. Development and evolution of body form and limb reduction in squamates: A response to Sanger and Gibson-Brown. Evolution 58:2107–2108.
- Wiens JJ, Slingluff JL. 2001. How lizards turn into snakes: A phylogenetic analysis of body form evolution in anguid lizards. Evolution 55:2303–2318
- Wiens JJ, Brandley MC, Reeder TW. 2006. Why does a trait evolve multiple times within a clade? Repeated evolution of snakelike body form in squamate reptiles. Evolution 60:123-141.
- Wise PAD, Russell AP. 2010. Development of the dorsal circumorbital bones in the leopard gecko (*Eublepharis macularius*) and its bearing on the homology of these elements in the Gekkota. Anat Rec 293:2001–2006.
- Zaher H, Apesteguía S, Scanferla CA. 2009. The anatomy of the upper cretaceous snake Najash rionegrina Apesteguía & Zaher, 2006, and the evolution of limblessness in snakes. Zool J Linn Soc 156:801–826.